

1 Seasonal and interannual variability of landfast sea ice in Atka Bay, 2 Weddell Sea, Antarctica

3 Stefanie Arndt¹, Mario Hoppmann¹, Holger Schmithüsen¹, Alexander D. Fraser^{2,3}, Marcel Nicolaus¹

4 ¹Alfred-Wegener-Institut Helmholtz-Zentrum für Polar- und Meeresforschung, 27570 Bremerhaven, Germany

5 ²Institute for Marine and Antarctic Studies, University of Tasmania, Hobart 7001, Tasmania, Australia

6 ³Antarctic Climate & Ecosystems Cooperative Research Centre, University of Tasmania, Hobart 7001, Tasmania, Australia

7 *Correspondence to:* Stefanie Arndt (stefanie.arndt@awi.de)

8 **Abstract.** Landfast sea ice (fast ice) attached to Antarctic (near-)coastal elements is a critical element of the local physical
9 and ecological systems. Through its direct coupling with the atmosphere and ocean, fast ice properties are also a potential
10 indicator of processes related to a changing climate. However, in-situ fast-ice observations in Antarctica are extremely
11 sparse because of logistical challenges and harsh environmental conditions. Since 2010, a monitoring program observing the
12 seasonal evolution of fast ice in Atka Bay has been conducted as part of the Antarctic Fast Ice Network (AFIN). The bay is
13 located on the north-eastern edge of Ekström Ice Shelf in the eastern Weddell Sea, close to the German wintering station
14 Neumayer III. A number of sampling sites have been regularly revisited between annual ice formation and breakup each year
15 to obtain a continuous record of sea-ice and sub-ice platelet-layer thickness, as well as snow depth and freeboard across the
16 bay.

17 Here, we present the time series of these measurements over the last nine years. Combining them with observations from the
18 nearby Neumayer III meteorological observatory as well as auxiliary satellite images enables us to relate the seasonal and
19 interannual fast-ice cycle to the factors that influence its evolution.

20 On average, the annual consolidated fast-ice thickness at the end of the growth season is about two meters, with a loose
21 platelet layer of four meter thickness beneath, and 0.70 meter thick snow on top. Results highlight the predominately
22 seasonal character of the fast-ice regime in Atka Bay without a significant interannual trend in any of the observed variables
23 over the nine-year observation period. Also, no changes are evident when comparing with sporadic measurements in the
24 1980s and 90s. However, strong easterly winds in the area govern the year-round snow redistribution and also trigger the
25 breakup of fast ice in the bay during summer months.

26 Due to the substantial snow accumulation on the fast ice, a characteristic feature is frequent negative freeboard, associated
27 flooding of the snow/ice interface, and a likely subsequent snow ice formation. The buoyant platelet layer beneath negates
28 the snow weight to some extent, but snow thermodynamics is identified as the main driver of the energy and mass budgets
29 for the fast-ice cover in Atka Bay.

30 The new knowledge of the seasonal and interannual variability of fast-ice properties in the present study helps to improve
31 our understanding of interactions between atmosphere, fast ice, ocean and ice shelves in one of the key regions of Antarctica,
32 and lays the foundation for more multi-disciplinary studies in this region.

33 **1 Introduction**

34 The highly dynamic pack ice of the open polar oceans is continuously in motion under the influence of winds and ocean
35 currents (Kwok et al., 2017). In contrast, landfast sea ice (short: fast ice) is attached to the coast or associated geographical
36 features, such as for example a shallow seafloor (especially in Arctic regions) or grounded icebergs, and is therefore
37 immobile (JCOMM Expert Team on Sea Ice, 2015). Fast ice is a predominant and characteristic feature of the Arctic
38 (Dammann et al., 2019; Yu et al., 2014) and Antarctic coasts (Fraser et al., 2012), especially in winter. Its seaward edge may
39 vary between just a few meters and several hundred kilometers from where it is attached to, mostly depending on the local
40 topography and coastline morphology. The main processes for fast-ice formation are either in-situ thermodynamic growth, or
41 dynamic thickening and subsequent attachment of ice floes of any age to the shore (Mahoney et al., 2007b).

42 In the Arctic, coastal regions that are characterized by an extensive fast-ice cover in winter are for example found in the
43 Chukchi Sea and Beaufort Sea (Druckenmiller et al., 2009; Mahoney et al., 2014; Mahoney et al., 2007a), the Canadian
44 Arctic (Galley et al., 2012), the East Siberian and Laptev Seas (e.g. Selyuzhenok et al., 2017), and the Kara Sea (Olason,
45 2016). While the fast-ice cover in these regions comes with its own particular impacts on the respective coastal systems,
46 what is common to them is that they have undergone substantial changes in recent decades (Yu et al., 2014). These include a
47 reduction of fast-ice area (Divine et al., 2003), later formation and earlier disappearance (Selyuzhenok et al., 2015) and a
48 reduction of thickness (Polyakov et al., 2003).

49 Along the Antarctic coastline, the fast-ice belt extends even further from the coast (Fraser et al., 2012; Giles et al., 2008) due
50 to the presence of grounded icebergs in much deeper waters of up to several hundred meters (Massom et al., 2001a).
51 Embayments and grounded icebergs provide additional protection against storms and currents, and are often favorable for
52 the formation of a recurrent and persisting fast-ice cover (Giles et al., 2008). Fast-ice around Antarctica is still usually
53 seasonal rather than perennial, and reaches thicknesses of around 2 meters (Jeffries et al., 1998; Leonard et al., 2006),
54 although it may attain greater ages and thicknesses in some regions (Massom et al., 2010). It mostly forms and breaks up
55 annually as a response to various environmental conditions, such as heavy storms (Fraser et al., 2012; Heil, 2006). Its
56 immediate response to both local atmospheric conditions and lower latitude variability of atmospheric and oceanic
57 circulation patterns via the respective teleconnections (Aoki, 2017; Heil, 2006; Mahoney et al., 2007b) make fast ice a
58 sensitive indicator of climate variability and even climate change (Mahoney et al., 2007a; Murphy et al., 1995). Based on the
59 complexity and significance of fast ice in the Antarctic climate system, there is an urgent need for prognostic Antarctic fast
60 ice in regional models, and later in global climate models, to capture its potential major impacts on the global ocean
61 circulation, as developed recently for the Arctic (Lemieux et al., 2016).

62 Although fast ice only represents a rather small fraction of the overall sea-ice area in Antarctica (Fraser et al., 2012), it may
63 contribute significantly to the overall volume of Antarctic sea ice, especially in spring (Giles et al., 2008). The presence and
64 evolution of Antarctic fast ice is often associated with the formation and persistence of coastal polynyas, regions of
65 particularly high sea-ice production (Fraser et al., 2019; Massom et al., 2001a; Tamura et al., 2016; Tamura et al., 2012) and
66 Antarctic Bottom Water formation (Tamura et al., 2012; Williams et al., 2008). Also, it forms an important boundary
67 between the Antarctic ice sheet and the pack ice/ocean, for example prolonging the residence times of icebergs (Massom et
68 al., 2003), mechanically stabilizing floating glacier tongues and ice shelves, and delaying their calving (Massom et al., 2010;
69 Massom et al., 2018). Therefore, one particularly interesting aspect of Antarctic fast ice is its interaction with nearby ice
70 shelves, floating seaward extensions of the continental ice sheet that are present along nearly half of Antarctica's coastline.
71 Under specific oceanographic conditions, supercooled Ice Shelf Water favors the formation of floating ice crystals within the
72 water column (Foldvik, 1977), as opposed to the regular process of sea-ice formation by heat transport from the ocean
73 towards the colder atmosphere. These crystals may be advected out of an ice-shelf cavity and rise to the surface (Hoppmann
74 et al., 2015b; Mahoney et al., 2011; Hughes et al., 2014). They are eventually trapped under a nearby fast-ice cover and may
75 accumulate in a layer reaching several meters in thickness (Gough et al., 2012; Price et al., 2014; Brett et al., 2020). This
76 sub-ice platelet layer has profound consequences for the local sea-ice system, and forms an entirely unique habitat.
77 Thermodynamic growth of the overlying solid fast ice into this layer (by heat conduction from the ocean into the
78 atmosphere) leads to subsequent consolidation, and the resulting incorporated platelet ice may contribute significantly to the
79 local fast-ice mass and energy budgets. This phenomenon has been documented at various locations around Antarctica
80 (Langhorne et al., 2015 and references therein), and where present, is a defining feature of the local coastal system. Refer to
81 (Hoppmann, in review) for a comprehensive review of platelet ice.

82 The effects of fast ice on the exchange processes between ocean and atmosphere are further amplified by the accumulation
83 of snow, as it forms a thick layer over large portions of the Antarctic sea ice (Massom et al., 2001b). However, the snow
84 cover has opposing effects on the energy and mass budgets of sea ice in the region. On the one hand, due to its low thermal
85 conductivity, snow acts as a barrier to heat transfer from sea ice to the atmosphere and effectively reduces ice growth at the
86 bottom (Eicken et al., 1995). On the other hand, snow contributes significantly to sea-ice thickening at the surface through
87 two distinct seasonal processes: snow-ice and superimposed ice formation. In winter/spring, the heavy snow load leads to the
88 depression of the sea-ice surface below water level, causing flooding of the snow/ice interface. The subsequent refreezing of
89 the snow/water mixture forms a salty layer of so-called snow-ice (e.g. Eicken et al., 1994; Jeffries et al., 1998; 2001). In
90 contrast, in summer internal snowmelt leads to melt water percolating to the snow/ice interface where it refreezes and forms
91 fresh superimposed ice (Haas, 2001; Haas et al., 2001; Kawamura et al., 2004). Both processes contribute significantly to
92 sea-ice growth from the top, and thus to the overall sea-ice mass budget in the Southern Ocean.

93 Beyond its contribution to the general sea-ice mass and energy budget in the Southern Ocean, fast ice also plays an important
94 role for the ice-associated ecosystem, as it provides a stable habitat for microorganisms (e.g. Günther and Dieckmann, 1999)
95 and serves as a breeding ground for, e.g., Weddell seals and Emperor penguins (Massom et al., 2009).

96 Fast ice and its properties as described above have been studied around Antarctica for a long time, especially related to
97 logistical work at the summer and overwintering bases close to the coast of the continent. In order to commonly coordinate
98 and facilitate this research, and thus establish an international network of fast-ice monitoring stations around the Antarctic
99 coastline, the international Antarctic Fast Ice Network (AFIN) was initiated during the International Polar Year (IPY)
100 2007/2008 (Heil et al., 2011). Active international partners are, e.g., Australia and China working at Davis Station and
101 Zhongshan Station on the eastern rim of Prydz Bay in East Antarctica (Heil, 2006; Lei et al., 2010), New Zealand working
102 out of Scott Base in McMurdo Sound in the Ross Sea (Langhorne et al., 2015, and references therein), Norway at the fast
103 ice in front of Fimbul Ice Shelf at Troll Station (Heil et al., 2011) and Germany in Atka Bay at Neumayer III (Hoppmann et
104 al., 2013), both in the vicinity of Dronning Maud Land. The regular, AFIN-related monitoring program at Neumayer III
105 started in 2010 in order to fill the observational gap in the Weddell Sea sector.

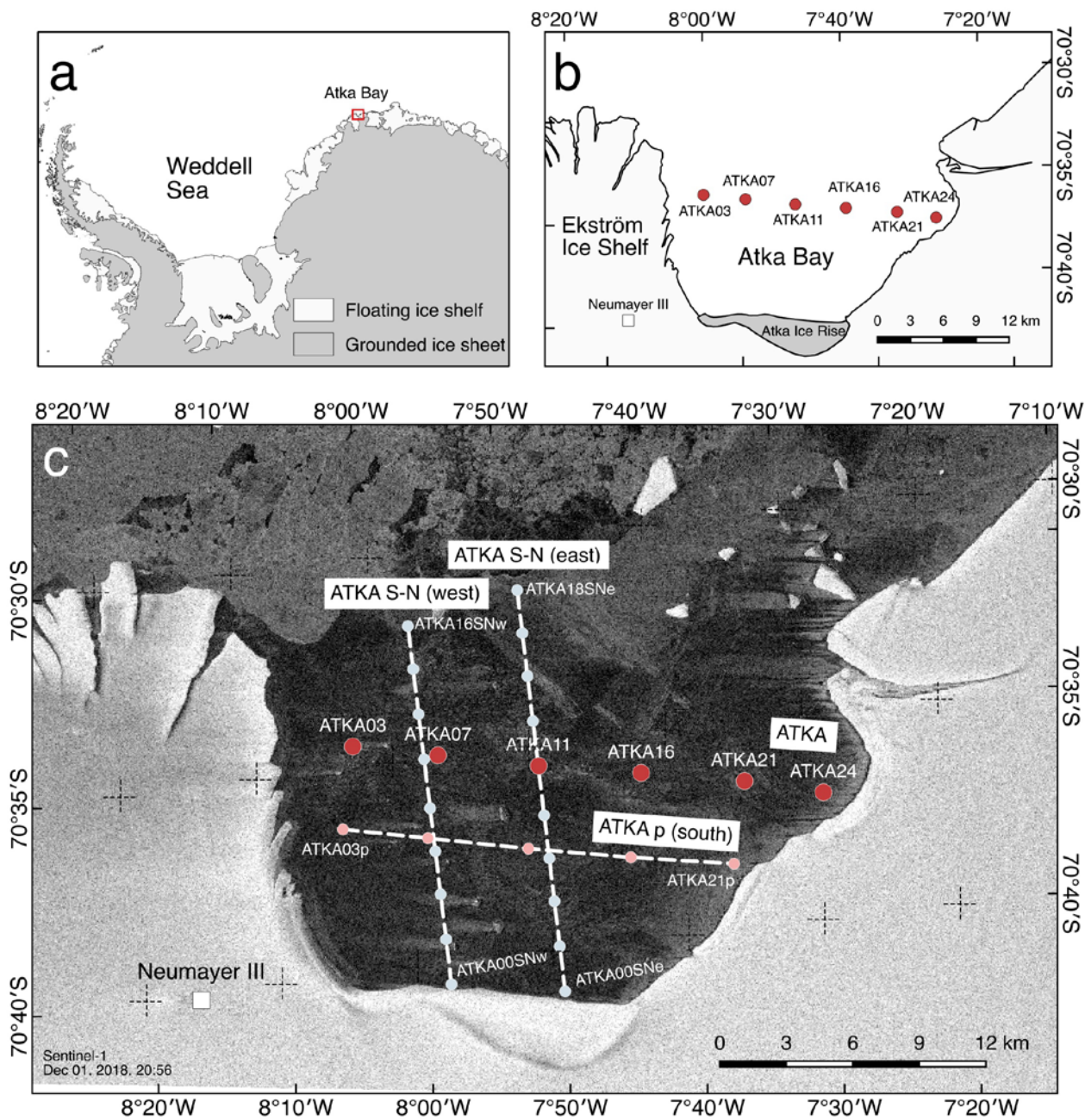
106 Here we present a decade of annual in-situ fast-ice observations in Atka Bay, which is one of the longest and most
107 continuous time series within AFIN so far. The main dataset is a record of fast-ice thickness, snow depth, freeboard, and
108 sub-ice platelet-layer thickness that was collected by a number of overwintering teams between 2010 and 2018. In addition
109 to determining the spatio-temporal variability of the fast-ice cover, we co-analyze this data with meteorological observations
110 and satellite imagery in order to determine how snow and platelet ice influence the local fast-ice mass budget. In doing so,
111 we aim to improve our understanding of the interaction between the atmosphere, fast ice, ocean and ice shelves in one of the
112 key regions in Antarctica.

113 **2 Study site and measurements**

114 **2.1 Study site: Atka Bay**

115 The main study area of this paper is Atka Bay, an 18 km-by-25 km embayment in front of the Ekström Ice Shelf located on
116 the coast of Dronning Maud Land in the eastern Weddell Sea, Antarctica, at 70°35'S/ 7°35'W (Figure 1). Atka Bay is
117 flanked towards the east, south and west by the edges of the ice shelf which rise as high as 20 meters above sea level. The
118 cavity geometry of the Ekström Ice Shelf is one of the best known in Antarctica (Smith et al., 2020). Atka Bay is seasonally
119 sea-ice covered, and the water depth ranges between 100 and 500 m, with a steep canyon of 275 m depth in the central bay
120 (Kipfstuhl, 1991). Since the 1980s, when the first German research station Georg-von-Neumayer Station was established in
121 the region, a variety of measurements has been carried out in the bay. Today's German research station Neumayer III is
122 located at a distance of about 8 km from the bay, where drifting snow regularly forms natural ramps between the sea ice and
123 the ice-shelf surface. Prior investigations of the interactions between ice shelf, sea ice and ocean in the bay and its
124 surroundings have been carried out by Kipfstuhl (1991) and Nicolaus and Grosfeld (2004), as well as more recently by
125 Hoppmann et al. (2015a) and Hoppmann et al. (2015b). Ecosystem studies from the 1990's have been published by Günther
126 and Dieckmann (1999); Günther and Dieckmann (2001) and Günther and Dieckmann (2001).

127



129

130 **Figure 1.** Overview of the study site and its surroundings. (a) Atka Bay (red marker) is located at the edge of the

131 northeastern Weddell Sea. Coastline data taken from SCAR Antarctic Digital Database. (b) Close-up of map (a) to focus on

132 the study site of Atka Bay. The sampling sites of the standard transect (ATKA) are marked with red circles. (c) Enlargement

133 of (b) showing in addition to the standard transect (red circles) the parallel transect in the south (ATKA p; light red circles)
134 from ATKA03p to ATKA21p as well the eastern and western perpendicular transects ATKA S-N (east) from ATKA00SNe
135 to ATKA18SNe and ATKA S-N (west) from ATKA00SNw to ATKA16SNw, each with a distance of 2 kilometers between
136 adjacent sampling sites (light blue circles). The southern, eastern and western transects were sampled during a field
137 campaign between November and December 2018. Background: Copernicus Sentinel data 01 December 2018, processed by
138 ESA.

139 **2.2 Sea-ice conditions**

140 Atka Bay is seasonally covered with sea ice that is attached to the ice shelf to form immobile fast ice. Following the method
141 of fast-ice time series retrieval detailed in Fraser et al. (2019), we obtained year-round estimates of fast-ice extent in Atka
142 Bay from MODIS visible and thermal infrared satellite imagery. Hence, the fast-ice extent time series presented here is a)
143 produced at a 1 km spatial and 15 day temporal resolution, from 15-day MODIS cloud-free composite images (following
144 Fraser et al., 2010) and edge-detected non-cloud-filtered composite images; b) spans the time period from March 2000 to
145 March 2018; and c) is semi-automated in the sense that the fast-ice edge is automatically delineated during times of high
146 contrast to offshore pack ice/open water, and manually delineated at other times.

147 Accordingly, the initial ice formation in the bay has started in March in recent years (Figure 2), with persistent easterly
148 winds forcing increased dynamic sea-ice growth towards the western ice-shelf edge of the bay. Once the bay is completely
149 covered by fast ice usually at the end of April (Figure 2), further in-situ ice growth takes place. In the following summer, the
150 ice does not melt in-situ, but breaks up and drifts out of the bay once the conditions are sufficiently unstable. Stabilization
151 and breakup of the ice-covered bay depend on the presence/absence of pack ice offshore of Atka Bay associated with
152 changing ocean currents and winds, as well as stationary and passing icebergs. Thus, fast-ice breakup in the bay starts
153 usually in December/January after the pack ice in front of the fast ice has retreated (Figure 2).

154 During our study period from 2010/2011 to 2018/19, there were two exceptions to this “typical” annual cycle: In September
155 2012, a large iceberg (generally referred to as “B15G”) grounded in front of Atka Bay, sheltering the fast ice and
156 consequently preventing sea-ice breakup in the following summer (Hoppmann et al., 2015b), resulting in second-year fast
157 ice in the bay in 2013. A year later, in August 2013, the iceberg dislodged itself, drifting westwards following the Antarctic
158 Coastal Current. Fragments of the iceberg remained grounded in the northern part of the bay, causing it to be blocked again
159 two years later, and therefore preventing sea-ice breakup in austral summer 2014/2015 for a second time within the study
160 period. The iceberg fragments became mobile during the course of the following year, resulting in the bay to become ice-free
161 again in the following summer.

162

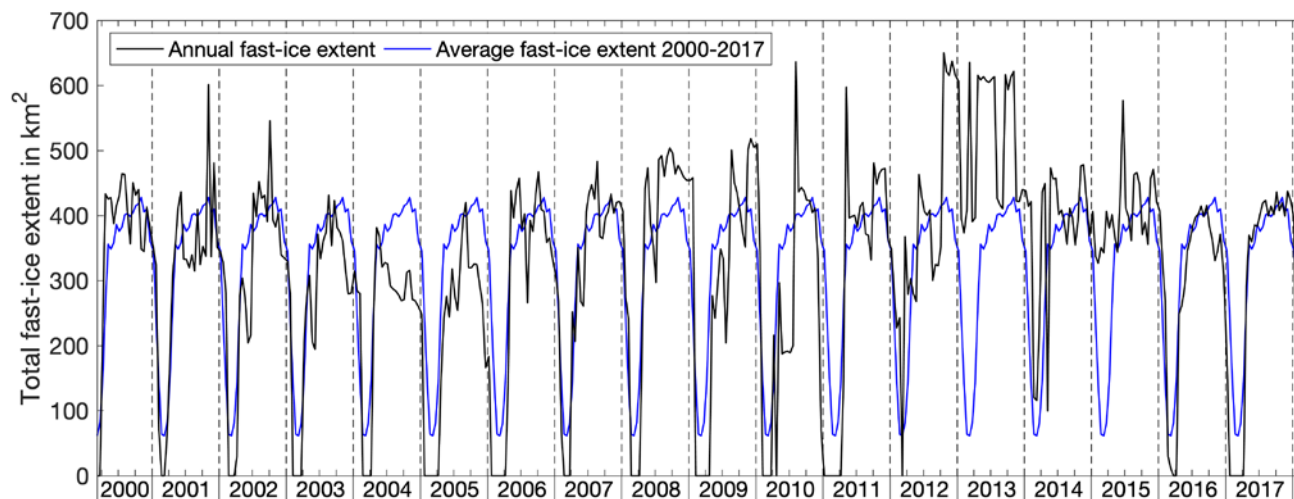


Figure 2: Time series of fast-ice extent in Atka Bay between 8° 12'W and 7° 24'W derived from MODIS data between early 2000 to early 2018 (black line). The blue line shows the annual mean extent repeated over the same time period. The average fast-ice extent over the entire time series is $319.2 \pm 167.8 \text{ km}^2$, with an uncertainty of 86.6 km^2 .

2.3 Sea-ice measurements across Atka Bay

Since 2010, the AFIN monitoring protocol has been implemented to study the seasonal evolution of fast ice along a 24-km long west-east transect in Atka Bay (“standard transect”, red circles in Figure 1). Here, six sampling sites have been regularly revisited between annual sea-ice formation and breakup each year to obtain a continuous record of snow depth, freeboard, sea ice- and sub-ice platelet-layer thickness across the bay (Arndt et al., 2019). Sampling sites on the standard transect are referred to in this paper as ATKAx_x, where xx represents the distance in kilometers to the ice-shelf edge in the west.

Generally, measurements along that standard transect are carried out once a month by the wintering team usually between June and January, when safe access to the sea ice is possible. At each sampling site, up to five measurements are taken in an undisturbed area, one as the center measurement and four more at a distance of approx. 5 meters in each direction, in order to account for the spatial variability of sea-ice and snow properties. In years of prevailing second-year ice in the bay (2012/2013, 2014/2015), the number of observations per sampling site was reduced to one (the center measurement) due to exceptionally thick snow and ice. Throughout this manuscript, we mainly present the mean values from those up to five single measurements per sampling site. While all measurements along the standard transect from 2010/2011 to 2018/2019 are included in this study, the sea-ice monitoring activities will be continued beyond this work.

In November and December 2018, additional measurements in both, parallel and perpendicular transect lines to the standard transect, have been performed (Figure 1c). Sampling sites on parallel transects are referred to in this paper as ATKAx_{xp},

185 where xx represents the distance in kilometers to the ice shelf edge in the west. Along the perpendicular western (w) and
186 eastern (e) transects from south to north, sampling sites are referred to in this paper as ATK AyySNw and ATK AyySNe,
187 where yy represents the distance in kilometers to the ice-shelf edge in the south.

188 Sea-ice and platelet-layer thickness as well as freeboard are measured with a (modified) thickness tape. In order to enable the
189 penetration of the usually semi-consolidated platelet layer, the regular metal plates at the bottom of the thickness tape were
190 replaced by a metal bar of ~2kg. The underside of the platelet layer is determined by gently pulling up the tape and
191 attempting to feel the first resistance to the pulling. Sea-ice thickness was measured either by pulling this modified tape
192 through the entire platelet layer until the solid sea-ice bottom is reached (with a high risk of it getting stuck), or using a
193 regular ice thickness tape. The modified tape is retrieved by pulling a small rope attached to one side of the metal bar. Snow
194 depth was measured using ruler sticks. Freeboard is defined as the distance between the snow/ice interface and the sea-water
195 level, while the snow/ice interface above (below) sea-water level is referred to as positive (negative) freeboard.

196 In order to determine the influence of snow and the underlying platelet layer to the observed freeboard (F), we also
197 calculated this parameter, assuming a hydrostatic equilibrium for floating snow-covered sea ice with an additional buoyancy
198 (the platelet layer below), using Archimedes' principle:

$$199 \quad F = - \frac{I \cdot (\rho_I - \rho_W) + S \cdot \rho_S + P \cdot (\rho_P - \rho_W)}{\rho_W}, \quad (\text{Eq. 1})$$

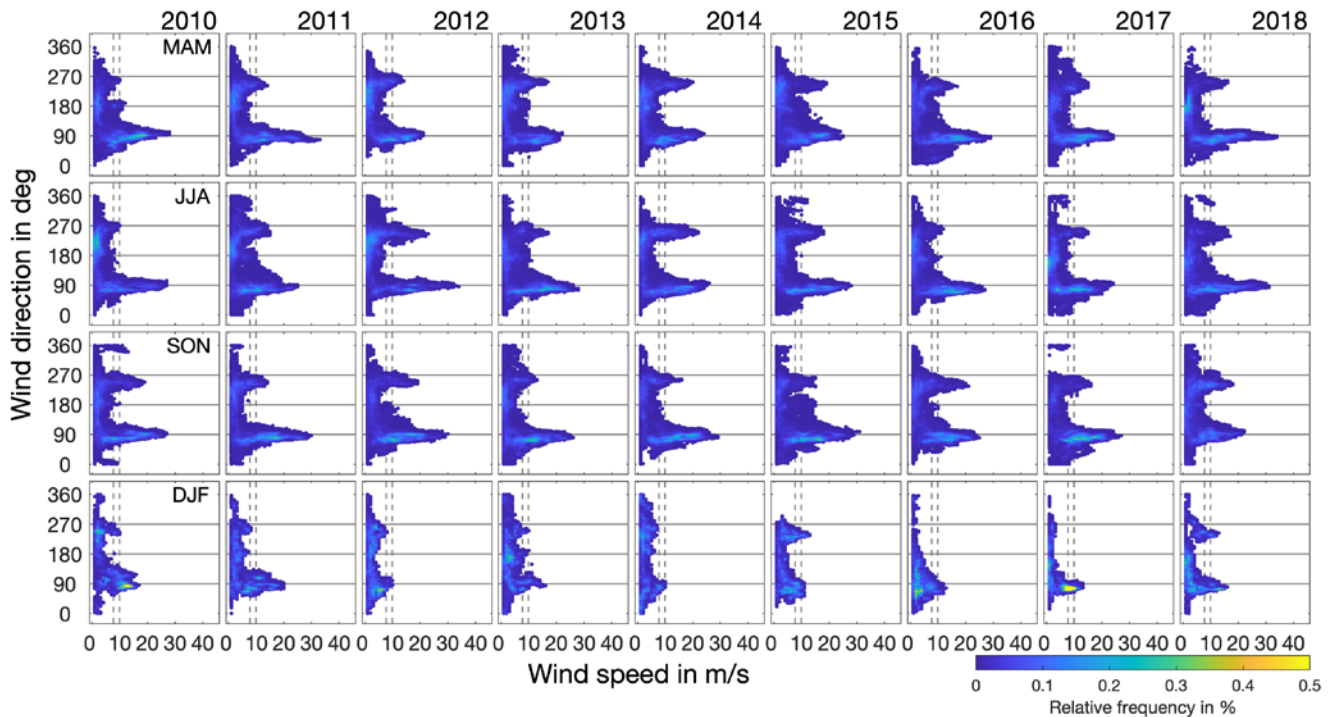
200 where I refers to sea-ice thickness, S to snow depth, P to platelet-layer thickness, the indices I refers to sea ice, S to snow, P
201 to the platelet layer, and W to water. Constant typical densities of $\rho_W = 1032.3 \text{ kg m}^{-3}$, $\rho_S = 330 \text{ kg m}^{-3}$ and $\rho_I = 925 \text{ kg m}^{-3}$
202 are assumed in this study. The platelet-layer density ρ_P is calculated as the product of sea-ice density and platelet-layer ice
203 volume fraction β . In this study, we used a constant ice-volume fraction of $\beta = 0.25$, as suggested by Hoppmann et al.
204 (2015b).

205 The described bore-hole measurements are occasionally complemented by additional total (sea-ice plus snow) thickness
206 measurements with a ground-based electromagnetic induction instrument (e.g. Hunkeler et al., 2016) as well as autonomous
207 ice tethered systems, such as Ice Mass balance or Snow Buoys (Grosfeld et al., 2015; Hoppmann et al., 2015a). However,
208 this paper focusses on the regular bore-hole measurements only, as the additional observations address scientific questions
209 beyond the scope of this paper.

211 **2.4 Meteorological conditions and observations at Neumayer III**

212 At the meteorological observatory of the nearby wintering base Neumayer III, atmospheric conditions have been recorded
213 since 1981 (König-Langlo and Loose, 2007), including the study period from 2010/2011 to 2018/19, and continuing beyond
214 it (Schmithüsen et al., 2019). Occasionally, automatic weather stations (AWS) were temporarily installed on the sea ice to
215 record the meteorological conditions directly on the sea ice (Hoppmann et al., 2015a). Since the 2m air temperature and the
216 wind velocity at the meteorological observatory and the AWS on the ice showed a fairly good agreement in prior studies

217 (Hoppmann et al., 2015a; Hoppmann et al., 2013), we utilize in this paper the more continuous records of the meteorological
 218 observatory in order to investigate the links between sea-ice conditions and atmospheric conditions. The Neumayer III data
 219 is recorded as minutely averages of typically 10 values per averaging interval. The instrumentation is checked on a daily
 220 basis, any erroneous values, e.g. caused by riming or instrument failure, are removed from the record. Therefore, the data
 221 quality can be considered high, even though there might be gaps in the records due to the validation routines. Nevertheless,
 222 data availability is 99.4% for wind direction, 99.0% for wind speed and 99.7% for air temperature. Uncertainties are
 223 essentially those classified by the manufacturers. Instrument details are given in the metadata of the datasets since February
 224 2017 in Schmithüsen et al. (2019), earlier data is documented in König-Langlo and Loose (2007).
 225 Generally, in the vicinity of Neumayer III the weather is strongly influenced by cyclonic activities which are dominated by
 226 easterly moving cyclones north of the station. This leads to prevailing persistent and strong easterly winds which exhibit a
 227 seasonal cycle with strongest winds during winter time (Figure 3). The second strongest mode in the wind direction
 228 distribution at 270° (westward) is associated with super geostrophic flows resulting from a high-pressure ridge north of
 229 Neumayer III (König-Langlo and Loose, 2007). These strong winds lead to frequent drifting and blowing snow. Here, we
 230 expect snow transport for 10-m wind velocities exceeding 7.7 m/s for dry snow and exceeding 9.9 m/s for wet snow (Li and
 231 Pomeroy, 1997).
 232



233
 234 **Figure 3:** Distribution of wind speed related to wind directions separated for austral fall (March, April, May; MAM), winter
 235 (June, July, August; JJA), spring (September, October, November; SON), and summer (December, January, February; DJF)

236 for the study period from 2010 to 2018. Colors indicate the relative frequency of each shown value pair. Dashed vertical
237 lines denote thresholds for 10-m wind speeds for snow transport of dry (7.7 m/s) and wet snow (9.9 m/s) (Li and Pomeroy,
238 1997).

239 **3 Results**

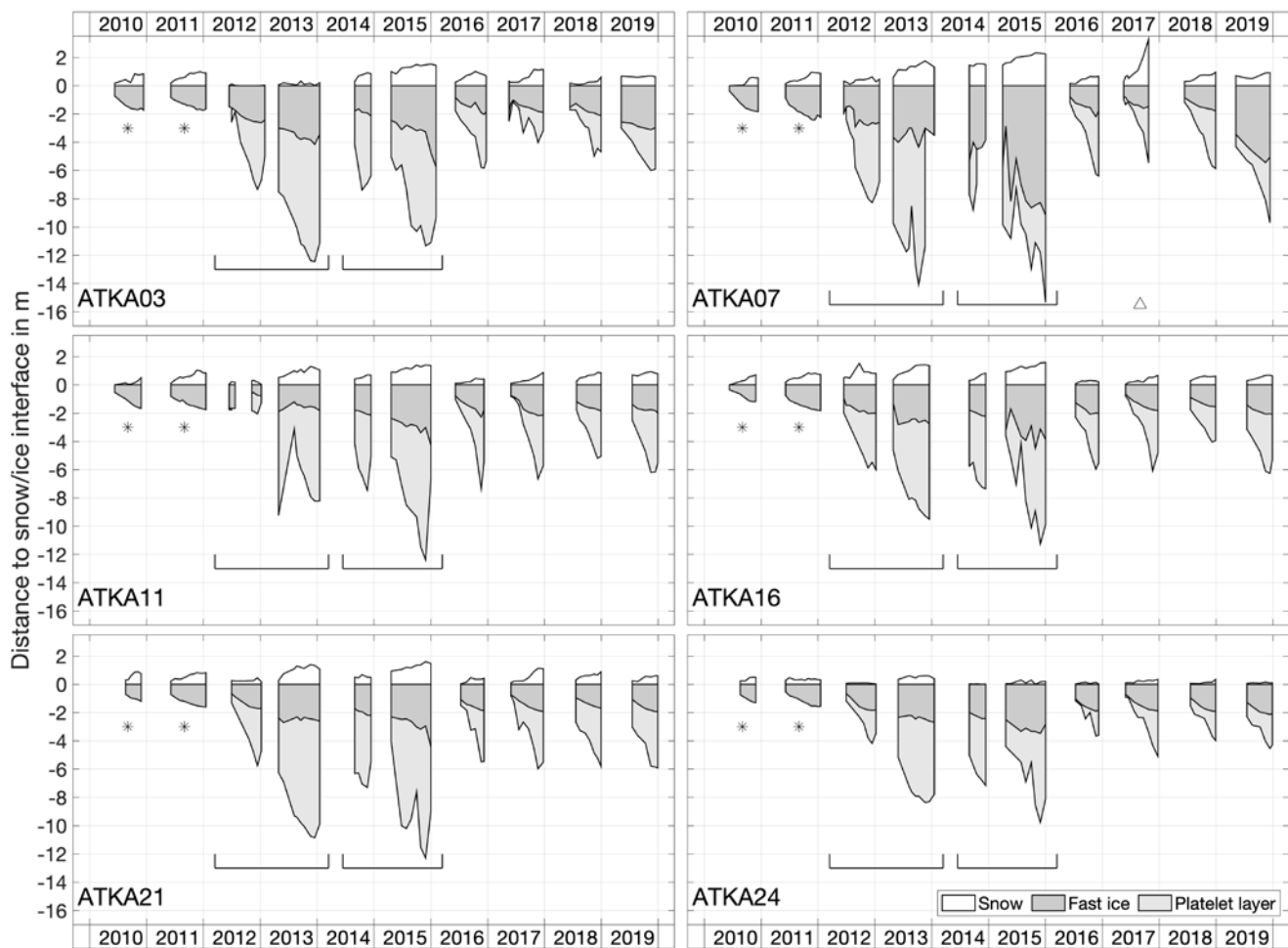
240 **3.1 Nine-year record of sea-ice and platelet-layer thickness, snow depth and freeboard along a 24-km W-E transect**

241 Figure 4 summarizes all conducted measurements of snow depth, sea-ice and platelet-layer thickness on the standard transect
242 from bore-hole measurements for each ATKA sampling site in the study period from 2010 to 2018. In the seven months
243 when sea-ice conditions allowed safe access (usually from May/June to December), about eight sets of measurements were
244 taken along the standard transect crossing Atka Bay, i.e. once every three to four weeks.

245 Analyzing the average annual maximum values of the investigated parameters (Table 1) for years of seasonal fast ice only
246 (excluding 2013 and 2015) and neglecting local iceberg disturbances (ATKA07 in 2017), the highest annual snow
247 accumulation of 0.89 ± 0.36 m was measured at ATKA07, while the smallest by far was measured at ATKA24 at the
248 easternmost sampling site, with only 0.28 ± 0.19 m. Averaged over the entire bay, the lowest snow accumulation of $0.51 \pm$
249 0.30 m was observed in 2016. In contrast, 2011 was the year with the most snow and an average snow depth of 0.85 ± 0.20
250 m across the bay. The average seasonal fast-ice thickness based on the measurements during the observation period varied
251 between 1.74 ± 0.31 m (ATKA21) and 2.58 ± 1.28 m (ATKA07) with a mean value of 1.99 ± 0.63 m. The underlying
252 seasonal platelet layer reached an average annual thickness of 3.91 m, which, however, shows a strong gradient in the
253 average annual maximum values (Table 1) from 4.62 ± 0.67 m at ATKA07 in the west of the bay to 2.82 ± 1.20 m at
254 ATKA24 in the east.

255 In 2013 and 2015, the fast ice in Atka -Bay became second-year ice due to grounded icebergs in front of the bay. Within the
256 respective second year, snow depth increased further by an additional 0.88 ± 0.43 in 2013 and by 0.74 ± 0.27 m in 2015. In
257 2013, the average fast-ice thickness across the bay increased by an additional 1.21 ± 0.42 m, while in 2015, it increased by
258 an additional $2.79 \text{ m} \pm 1.48$ m. In the years of prevalent second-year ice in the bay, the thickness of the platelet layer
259 increased on average by $5.13 \text{ m} \pm 1.43$ m in 2013 (compared to the end of 2012), and $4.11 \text{ m} \pm 1.86$ m in 2015 (compared to
260 the end of 2014). During these periods, ATKA11 experienced the highest annual platelet-layer thickness increase of 6.82 m
261 and 6.44 m, respectively.

262



263

264

265

266

267

268

269

270

271

272

273

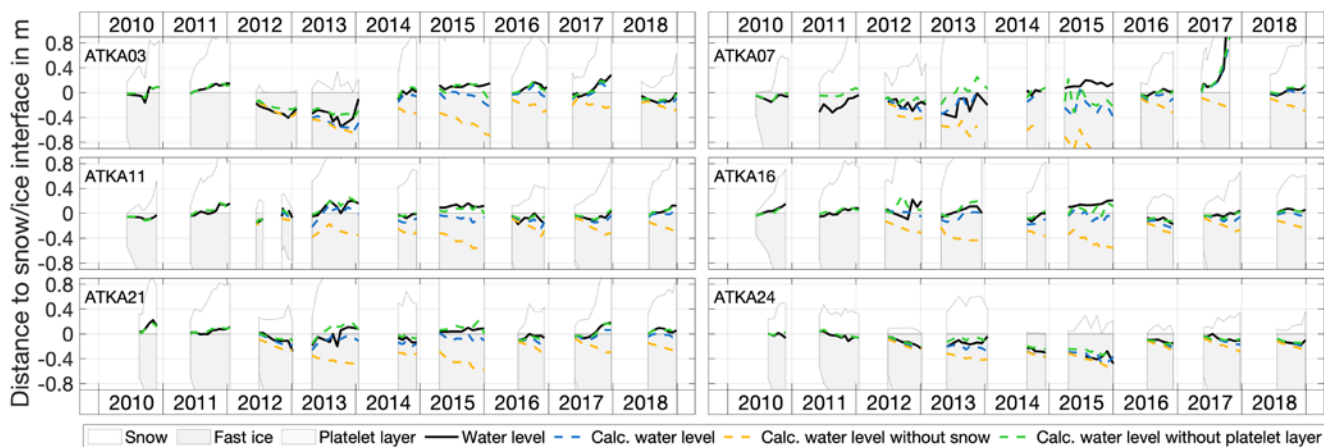
274

Figure 4: Time series of snow depth, fast-ice and platelet-layer thickness from bore-hole measurements along the standard transect for each ATKA sampling site (Figure 1) for the time period from 2010 to 2018. Note: In 2010 and 2011, the platelet-layer thickness was not measured (*). In 2012/2013 and 2014/2015 Atka Bay was blocked by icebergs, so the fast ice did not break up and turned into second-year ice instead (—). In 2017, a small iceberg in the vicinity of ATKA07 strongly influenced the snow measurements (Δ). Reference depth of 0 meters is the snow/ice interface.

Figure 5 depicts the evolution of the water level with respect to the snow/ice interface (which is the freeboard with an opposite sign) along the standard transect in the study period from 2010 to 2018. Taking all conducted freeboard measurements from seasonal fast ice into account, 55% reveal negative data, i.e. flooding can be assumed, with an average negative freeboard of -0.10 ± 0.08 m. In contrast, considering freeboard measurements from second-year ice only, 38% of the data indicate a negative freeboard, with an average of -0.22 ± 0.15 m. Analyzing the average annual maximum of the

275 negative freeboard values (Table 1) for years of seasonal fast ice only, and neglecting local iceberg disturbances (ATKA07
 276 in 2017), there is no distinct gradient across Atka Bay, but higher average negative freeboard values (-0.07 to -0.08 m) are
 277 recorded both in the far west (ATKA03) and in the east (ATKA16 and ATKA21), whereas the lowest average negative
 278 freeboard of -0.01 ± 0.08 m was measured at ATKA07. According to Equation 1, 89% of the calculated freeboard values are
 279 smaller than the measured values. The difference between measured and calculated freeboard values ranges from -0.19 to
 280 0.54 m with an average of 0.08 ± 0.10 m (towards higher measured value). Neglecting the underlying buoyant platelet layer
 281 in the calculation reduces the freeboard by 0.09 ± 0.06 m, whereas neglecting the snow layer on top of the sea ice increases
 282 the freeboard by 0.20 ± 0.17 m (Figure 5).

283



284

285 **Figure 5:** Close-up of Figure 4 which highlights the location of the water level with respect to the snow/ice interface (which
 286 has the opposite sign of the freeboard) as measured in the field (black solid line) and as calculated according to Equation 1
 287 including snow and platelet-layer thickness (blue dashed line), neglecting the snow cover (dashed yellow line) and platelet
 288 layer (dashed green line), respectively. Please note that, for the purpose of better illustration, we depict here the actual
 289 location of the water level rather than the freeboard (the only difference being the opposite sign). This means that, if the
 290 water level is above the snow/ice interface, this is depicted in the figure accordingly, while the actual freeboard carries a
 291 negative sign, and vice versa. The reference depth of 0 represents the snow/ice interface.

292

293 **Table 1:** Average annual maximum of snow depth, sea-ice and platelet-layer thickness, as well as freeboard (negative equals
 294 potential flooding) on the standard transect from bore-hole measurements for each ATKA sampling site (Figure 1) for the
 295 time period from 2010 to 2018, excluding years of second-year ice due to blocking of the bay (i.e. 2013 and 2015). ¹At
 296 ATKA11 all measurements of the year 2012 are also neglected as the ice has temporarily broken up again. ²At ATKA07 the
 297 snow measurements of the year 2017 are also neglected as a small iceberg has strongly influenced the accumulation rates.
 298 Standard deviations are given in brackets.

	ATKA03	ATKA07	ATKA11	ATKA16	ATKA21	ATKA24
Snow depth in m	0.81 (0.35)	0.89 (0.36) ²	0.74 (0.23) ¹	0.79 (0.37)	0.77 (0.24)	0.28 (0.19)
Ice thickness in m	2.04 (0.31)	2.58 (1.28)	1.97 (0.25) ¹	1.81 (0.36)	1.74 (0.31)	1.83 (0.35)
Platelet-layer thickness in m	3.88 (1.31)	4.62 (0.47)	4.59 (0.83) ¹	3.99 (0.94)	4.21 (0.54)	2.82 (1.20)
Freeboard in m	-0.08 (0.14)	-0.01(0.08) ²	-0.05(0.08) ¹	-0.07 (0.09)	-0.08 (0.10)	-0.05 (0.09)

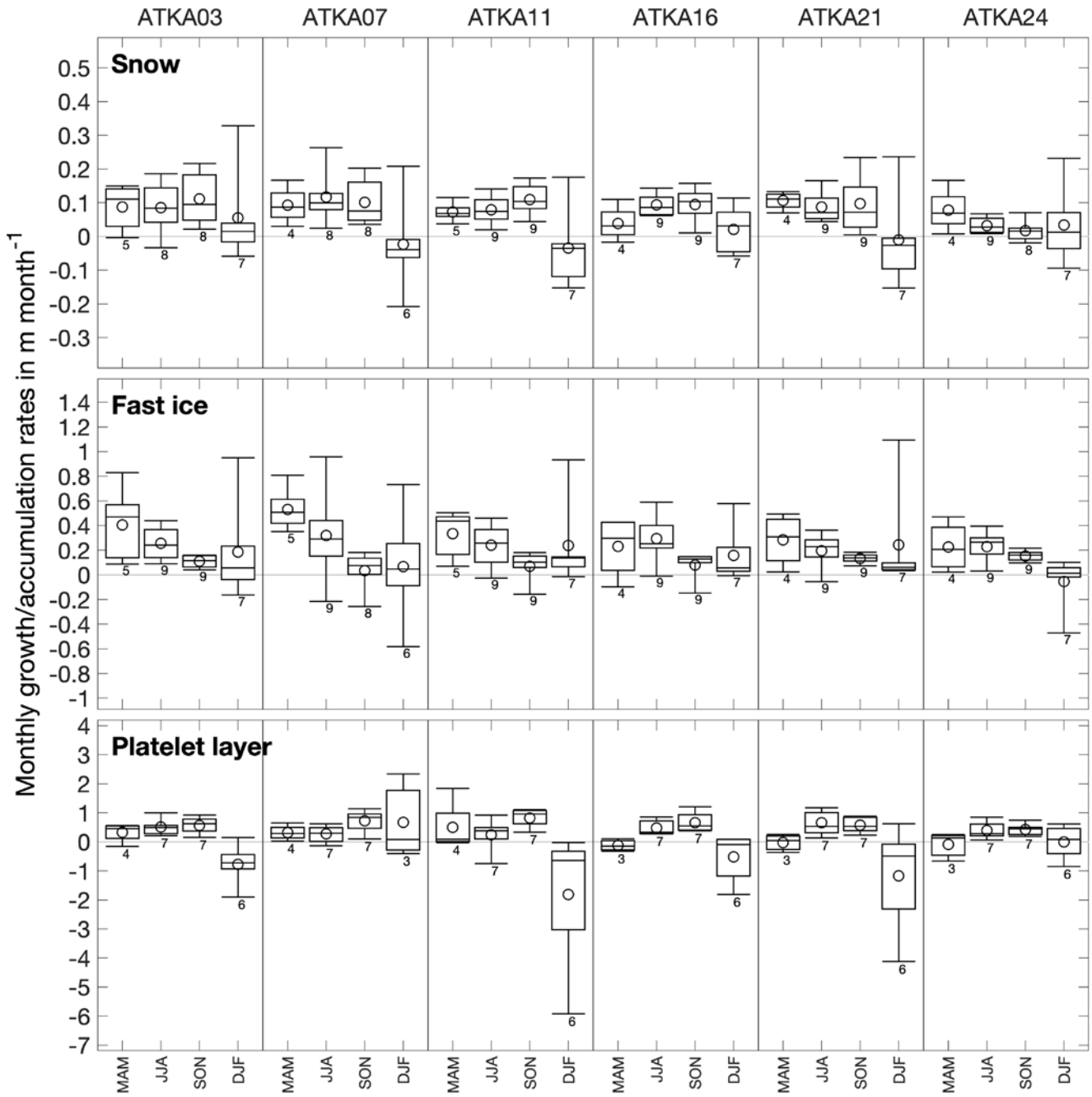
299
300

301 **3.2 Seasonal snow, sea-ice and platelet-layer accumulation/growth and melt rates**

302 Figure 6 summarizes the seasonal snow depth, sea-ice and platelet-layer thickness evolution separated for austral fall
303 (March, April, May; MAM), winter (June, July, August; JJA), spring (September, October, November; SON), and summer
304 (December, January, February; DJF) for each ATKA sampling point for the study period from 2010 to 2018.

305 Considering the average monthly snow accumulation rates, a slight increase from fall (from 0.04 to 0.09 m per month) to
306 spring (0.09 to 0.11 m per month) becomes apparent, if excluding the eastern sampling sites at ATKA21 and ATKA24.
307 Latter sampling sites show the highest monthly averaged accumulation rates during austral fall (0.11 and 0.08 m per month),
308 which subsequently decrease to 0.10 and 0.02 m per month, respectively. In contrast, a clear snow loss with a maximum
309 monthly average of up to 0.03 ± 0.12 m at ATKA11 and a maximum snow loss rate of 0.21 m per month at ATKA07 (80th
310 percentile), can be seen mostly during summer months. Also, the seasonal evolution of the platelet layer shows a similar
311 pattern: between austral autumn and spring, an average monthly thickness increase of up to 0.82 ± 0.30 m at ATKA11 is
312 observed. Excluding ATKA07, afterwards an average monthly platelet-layer thickness decrease of 0.85 m is calculated for
313 summer. The maximum decrease of 6.25 m per month occurred at ATKA11 in 2013 (80th percentile). However, it is highly
314 likely that this is a measurement error. In contrast, ATKA07 also reveals an increase in platelet-layer thickness during the
315 summer months with a monthly average of 0.67 ± 1.20 m. With regard to the growth rates of fast ice in Atka Bay, a
316 contrasting but expected seasonal development is observed: The highest average monthly fast-ice growth rates of up to
317 approx. 1 m per month (80th percentile) are measured in autumn, and decrease in the following month until spring. These
318 exceptionally high growth rates result from rapid growth of the solid fast ice into the (unconsolidated) sub-ice platelet layer,
319 i.e. from the subsequent freezing of the interstitial water between the platelets in the top part of the platelet layer. In other
320 words, some of the heat within the newly growing ice was already extracted earlier by the ocean during the process of
321 platelet crystal formation in the supercooled Ice Shelf Water plume. In the subsequent summer months, average monthly
322 sea-ice growth rates increased again to values between 0.07 m (ATKA07) and 0.24 m (ATKA21), except for ATKA24,

323 where sea-ice melt dominates with an average monthly melt rate of -0.05 ± 0.22 m and a maximum monthly sea-ice melt rate
 324 of -0.58 m.
 325

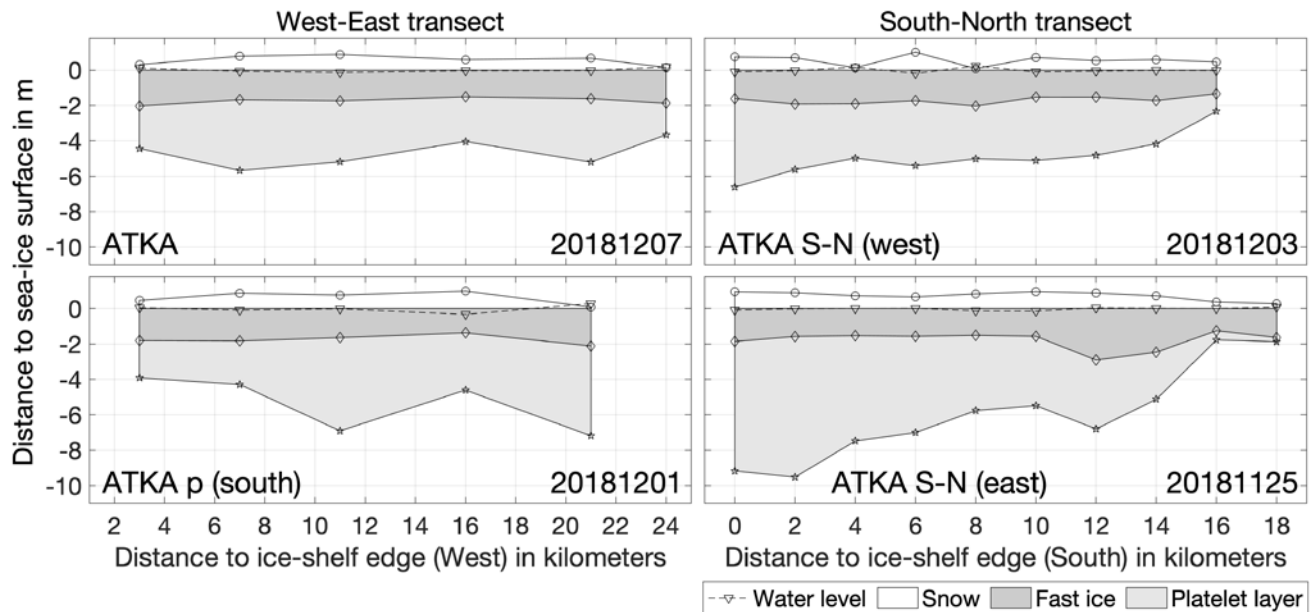


326

327 **Figure 6:** Seasonal snow, sea-ice and platelet-layer accumulation/growth and melt rates separated for austral fall (March,
328 April, May; MAM), winter (June, July, August; JJA), spring (September, October, November; SON), and summer
329 (December, January, February; DJF) for each ATKA sampling point for the study period from 2010 to 2018. Boxes are the
330 first and third quartiles; whiskers the 20th and 80th percentile. Circles indicate the mean, vertical lines in the boxes the
331 median. Numbers below the whiskers indicate the respective sampling size, i.e. the number of included years, with a
332 maximum of nine.
333

334 **3.3 Spatial variability of snow depth, sea-ice and platelet-layer thickness**

335 In order to describe the spatial variability of snow depth, sea-ice and platelet-layer thickness in west-to-east as well as in
336 south-to-north direction across Atka Bay, additional parallel and perpendicular transects to the standard transect have been
337 sampled in November/December 2018 (Figure 7). Considering the solid sea ice only, the complementary transect data show
338 that sea-ice thickness over the bay in south-north and west-east direction is rather constant with an average of 1.68 ± 0.21 m.
339 In contrast, neglecting the measurements in iceberg-affected areas, snow depth data show higher values in the south and in
340 the center of the bay of up to 1.00 ± 0.04 m, while decreasing significantly towards the eastern ice-shelf edge and northern
341 fast-ice edge to 0.08 ± 0.01 m and 0.28 ± 0.09 m, respectively. The platelet-layer thickness beneath the fast ice shows a large
342 spatial variability. While all measurements on the standard transect reveal the lowest platelet-layer thickness in the east of
343 the bay at ATKA24 (see Section 3.1), on the parallel transect in the south a maximum platelet-layer thickness of 7.18 ± 0.26
344 m at the easternmost sampling point (ATKA21p) is observed. For the perpendicular transects in south-to-north direction, a
345 significantly decreasing gradient in platelet-layer thickness from the ice-shelf edge towards the northern fast-ice edge is
346 evident. On the western south-to-north transect, a decrease from 6.62 ± 0.25 m to 2.33 ± 0.08 m was observed, whereas for
347 the eastern transect this strong gradient is even more apparent with a decrease from 9.17 ± 0.11 m to 1.88 ± 0.20 m.
348



349

350

351

352

353

354

355

356

Figure 7: Overview of measurements on the standard transect from west to east (upper left), the parallel one (lower left), the western perpendicular transect from south to north (upper right) and the respective parallel one to the east (lower right) showing the water level, snow depth, fast-ice and platelet-layer thickness across Atka Bay. All measurements were conducted between November 25, 2018 and December 07, 2018. For the parallel west-east transect (December 01, 2018), the platelet-layer thickness evolution is influenced by a nearby iceberg (see Figure 1c). Also, for the western north-south transect (December 03, 2018), snow measurements are influenced by several small icebergs in the vicinity between kilometers 4 and 8 (see Figure 1 c).

357

4 Discussion

358

4.1 Seasonal and interannual variability of snow depth, sea-ice and platelet-layer thickness

359

360

361

362

363

364

365

366

367

The fast-ice regime in Atka Bay is primarily seasonal and the sea-ice cover usually only remains in the bay if a breakup is prevented by grounded icebergs in front of it. For example, while in 2013 a 17km-by-10km iceberg (B15G) blocked the entire bay, in 2015, only small iceberg fragments of B15G in front of the bay were sufficient to ensure that the sea ice in the bay did not break up, but became perennial. It may also occasionally happen that small areas of fast ice remain attached to the ice-shelf edge, or that individual ice floes remain in the bay and are incorporated into the newly growing ice in the following winter. Not only does the presence and size of the icebergs play a role in the fast-ice seasonality, but also the location and associated influence of atmospheric circulation patterns and ocean processes.

Considering first of all the seasonal sea ice only, the presented measurements along the standard transect across Atka Bay indicate a clear seasonal cycle in all investigated variables, i.e. snow depth, sea-ice and platelet-layer thickness: The initial

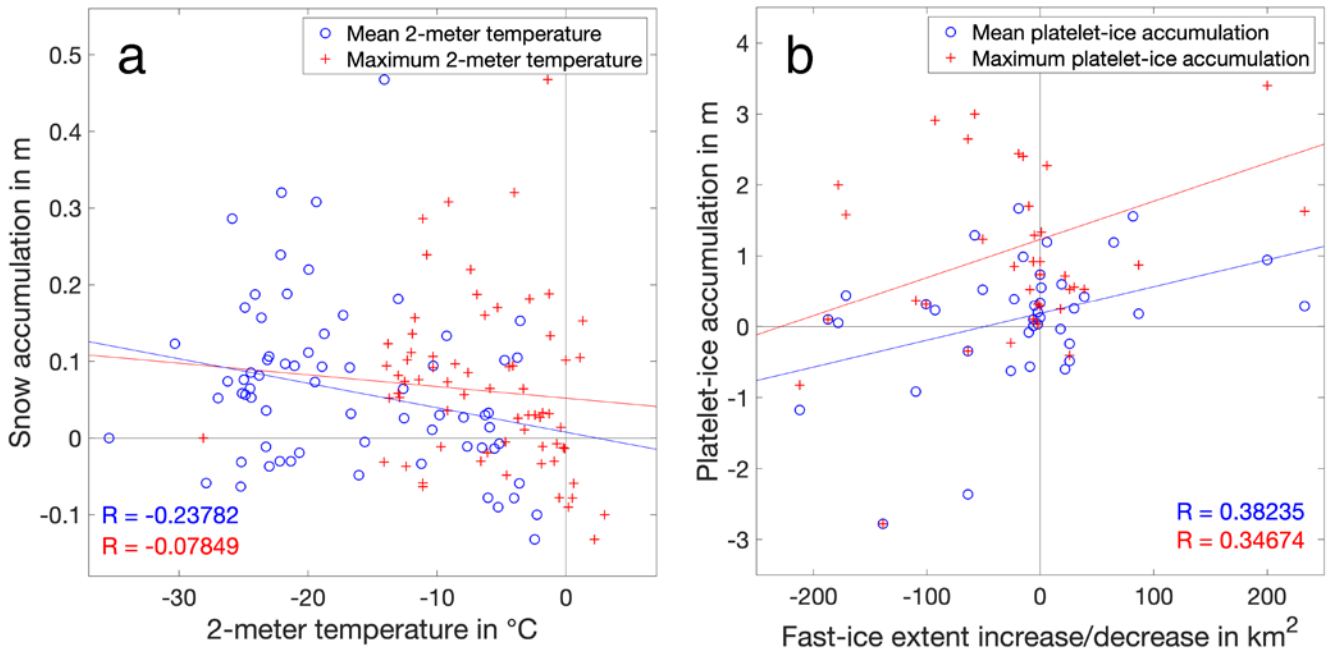
368 sea-ice formation in Atka Bay starts in March and proceeds towards a completely fast-ice-covered bay at the end of April.
369 The continuous sea-ice growth (i.e. ocean-atmosphere heat flux) proceeds with decreasing growth rate through fall and
370 winter until the thickening snow cover more and more reduces the heat flux between the upper ocean and the atmosphere,
371 preventing further thermodynamic sea-ice growth. However, the fast-ice thickness still increases in spring and even during
372 austral summer months (albeit very slowly). This can be explained by the measurement uncertainty with respect to the large
373 spatial variability of sea-ice thickness even on very small (centimeter) scales, but the consistency in the data suggests that it
374 could also be caused by consolidation processes within the platelet layer below, i.e. in-situ sea-ice growth by heat transport
375 into a supercooled plume residing right beneath the solid fast ice similar to observations in McMurdo Sound (Smith et al.,
376 2012; Leonard et al., 2011; Dempsey et al., 2010; Robinson et al., 2014). So far, in Atka Bay there is only evidence that
377 platelets grow quite large already while still suspended in the water column (Hoppmann et al., 2015b). To what degree an in-
378 situ growth of platelet crystals and consolidation processes that go beyond regular freeze-in of the topmost part of the
379 platelet layer by heat conduction to the atmosphere play a role at Atka Bay still needs to be investigated. In any case the
380 platelet layer is an efficient buffer between the fast ice and the incoming warmer water in summer (Eicken and Lange, 1989),
381 so the lack of noticeable fast-ice bottom melt is generally expected. Oceanographic (winter) data is sparse, and the
382 monitoring at Atka Bay has recently been extended to also include regular CTD casts, whenever the (challenging) conditions
383 and time constraints allow. An analysis of available CTD data in Atka Bay is currently ongoing, and will be shown in a
384 future dedicated study to close the above observational gaps with respect to the ocean.

385 Destabilization of the fast ice and the platelet layer below in summer is to a large extent driven by the presence/absence of
386 pack ice offshore Atka Bay. Thus, the initial breakup and subsequent retreat of the pack ice in front of the bay allow for
387 locally increasing ocean currents beneath the fast ice and the inflow of warm Antarctic Surface Water from the east
388 (Hoppmann et al., 2015a; Hattermann et al., 2012) causing both washing out of the platelet layer as well as mixing warm
389 water into the water column associated with a thinning rate of the platelet layer of approx. one meter per month from
390 December onwards. The retreating fast ice also initializes the sea-ice breakup in the bay starting usually in
391 December/January (Figure 2). The diminishing fast-ice zone goes along with an additional thinning of the platelet layer
392 (Figure 8 b) by, e.g., further washing out mechanisms. Even though the correlation between the change of fast-ice extent and
393 the mean (maximum) platelet-layer thickness between two consecutive surveys with a coefficient of 0.38 (0.35) is relatively
394 low, Figure 8 shows that decreasing platelet-layer thicknesses are generally associated with retreating fast ice in Atka Bay.
395 Also, Massom et al. (2018) have also shown that pack ice has a stabilizing effect as a buffer against ocean swells. The
396 deployment of complex oceanographic moorings, either ice- or seafloor-based, would help immensely to investigate ocean
397 properties and currents and their effect on sea ice and the ice shelf, but their deployment, and especially their recovery, is
398 extremely difficult and risky in the dynamic and harsh conditions of Atka Bay. While such deployments are logistically not
399 feasible at the moment, it is planned to include suitable instrumentation in the monitoring within the next years.

400 In contrast to the decrease in platelet-layer thickness beneath the fast ice in summer over the entire bay, the snow cover on
401 top does not show a clear seasonal pattern, but indicates a decrease in snow depth with increasing air temperature. However,

402 even in summer, no consistent snow melt with associated strong mass loss is observed over the entire bay. Rather, a strong
403 variability in snow depth over all sampling sites and all sampling years with a weak snow loss during summer months
404 (Figure 6) is observed. This pattern is a result of both, temporary temperatures above freezing which favor surface melting
405 (Figure 8a), and comparatively low wind speeds (Figure 3) preventing the accumulation of additional snow blown over from
406 the surrounding ice shelf. These results match well with results from studies on the seasonal cycle of snow properties in the
407 inner pack ice zone of the Weddell Sea as for example performed by Arndt et al. (2016), who also showed missing persistent
408 summer melt as highlighted above.

409 Overall, the 9-year time series for in-situ snow depth, sea-ice and platelet-layer thickness in Atka Bay do not show any trend
410 over the analyzed study period, whereas their inter-annual variability is dominated by local or temporary effects such as the
411 presence of icebergs, which may for example lead to small-scale strong snow accumulations (Figure 4) or occasionally even
412 to a perennial fast-ice regime. It is particularly remarkable that the average annual platelet-layer thickness increase of 4 m
413 (Table 1) is consistent with an earlier investigation at Atka Bay performed in 1982 by Kipfstuhl (1991) between the western
414 ice-shelf edge and ATKA03, and at the same time much higher than in another study from 1995, where a maximum platelet-
415 layer thickness of 1.5 m was measured in a similar location (Günther and Dieckmann, 1999). Considering the fact that these
416 two studies only sampled one site, the generally large spatial and temporal variabilities of platelet-layer properties, and the
417 results from our much more detailed study, we infer that there seems to be no clear trend over the past decades. Our results
418 are also in line with a recent study of Brett et al. (2020), who also found spatially highly variable platelet layers of 4+m
419 under fast ice in McMurdo Sound. Thereby, our results suggest that it is likely that the relevant (sub ice-shelf) processes in
420 this region have not changed much either. However, as already stated above, it is crucial to further look into all the available
421 oceanographic data that is available from the Atka Bay region in order to support (or disprove) these indications provided by
422 the fast-ice monitoring. Another benefit of such comparison would be to strengthen (or weaken) the hypothesis that fast-ice
423 properties can serve as an indicator for the status of an ice-shelf, as suggested by Langhorne et al. (2015)



424

425 **Figure 8:** Scatter plot comparing (a) the average 2-meter air temperature (see Section 2.4) and the snow accumulation
 426 between two consecutive surveys, and (b) increasing (positive values) and decreasing (negative values) fast-ice extent and
 427 platelet-layer thickness between two consecutive surveys. The analysis includes all measurements at all sampling sites
 428 throughout the study period from 2010 to 2018. Blue circles and red crossed denote the respective mean and maximum
 429 values within the time frame between the consecutive measurements. Colored solid lines in Figure (b) show the linear
 430 regression between both parameters with the respective correlation coefficients R .

431

432 4.2 Spatial variability of fast-ice properties related to the distance to the ice-shelf edges around the bay

433 When neglecting local disturbances, such as icebergs, our results clearly indicate differences in the evolution of platelet-
 434 layer thickness and snow depth with respect to the distance to the adjacent ice-shelf edges around Atka Bay. In contrast, the
 435 fast ice itself does not exhibit any large spatial variability, but measures at the end of the season a nearly uniform thickness
 436 of 2 meters across the bay, both in west-east and south-north direction (Figure 7).

437 Analysis of the spatial distribution of platelet-layer thickness under the fast ice along the standard transect over the entire bay
 438 reveals that ATKA24 shows a significantly thinner platelet layer than all other sampling sites. In contrast, the parallel
 439 transect towards the south reveals a significantly higher platelet-layer thickness at the sampling point closest to the eastern
 440 shelf ice edge (ATKA21p). Perpendicular sampling transects from close to the southern ice-shelf edge towards the fast-ice
 441 edge in the north show a strong increase of platelet-layer thickness near the ice-shelf edge, followed by a moderate decrease
 442 in platelet-layer thickness towards the north, which rapidly decreases about 5 kilometers off the fast-ice edge. This thickness

443 gradient is much more pronounced on the south-north transect in the central area of the bay compared to the western one.
444 Moreover, considering the entire time series of the west-east transect, the highest platelet-layer thickness is observed in the
445 central area of the bay (ATKA07 and ATKA11). Summarizing all these observations, we hypothesize that, on the one hand,
446 the strongest outflow of supercooled water from the ice-shelf cavity (along with associated suspended platelet crystals) leads
447 from the south centrally into the bay. On the other hand, local under-water topographic features of the ice shelf (i.e. ice rises)
448 at the eastern boundary of Atka Bay (Figure 1, Hoppmann et al., 2015b) might lead to a blocking of ocean currents and thus
449 the advection of suspended platelet crystals, causing the high platelet-layer thickness at ATKA21p and the consistently low
450 observed thickness north of this location at ATKA24 (Figure 4). The strongly decreasing gradient in the platelet-layer
451 thickness towards the northern sea-ice edge is likely due to increasing distance from the source of suspended platelet crystals
452 being advected from under the ice shelf and related washout effects. This is especially likely since at the time of the
453 corresponding measurement, the pack ice in front of the bay was already broken open, allowing for wind-induced currents
454 and locally solar-heated water (so-called mode 3 incursions, Jacobs et al. (1992) (Figure 1). Also, the fact that the
455 northernmost sampling points are located close the edge of the bay or even already outside of it, raises the probability that
456 the predominant coastal ocean current transports warm Antarctic Surface Water towards the fast-ice area, which would
457 further intensify this effect (Hattermann et al., 2012; Hoppmann et al., 2015b). From this, it can be generalized that a
458 smaller amount of platelet crystals can accumulate under narrow fast-ice areas, since these are exposed to stronger oceanic
459 currents and associated washout effects, as well as warm water incursions. Comparative analyses to other study regions are
460 not possible at this time, since, to our knowledge, no comparable transects were carried out so far in other Antarctic fast-ice
461 regions with platelet layers beneath. Regarding the properties of the ocean in this region with respect to its interaction with
462 the ice shelf and sea ice, Hoppmann et al., 2015b used a subset of oceanographic data collected by the nearby PALAOA
463 hydrographic observatory (Boebel et al., 2006) to link fast ice observations to ocean properties. A more recent study by
464 Smith et al. (2020) helped to constrain the boundary conditions for Ice Shelf Water outflow by mapping in great detail the
465 cavity geometry of the Ekström Ice Shelf. This study also shows data from repeated CTD casts through a borehole in the ice
466 shelf, revealing the buoyant outflow of Ice Shelf Water in a relatively shallow surface layer. While these efforts help to
467 better understand the complex system of ice shelf-ocean-sea ice interaction in this region, we conclude that a more
468 comprehensive, year-round oceanographic study that also implements a dedicated survey program is urgently needed as a
469 complement to the sea ice monitoring in order to investigate in more detail the outflow of Ice Shelf Water and the complex
470 processes involved in the redistribution of platelet crystals that emerge from the ice shelf cavity.

471 Examining the spatial distribution of snow over the bay, the considerably lower snow depth at ATKA24 compared to all
472 other sampling sites is striking, and most likely related to the proximity to the ice-shelf edge in approximately 1 km distance.
473 Due to the prevailing easterly winds in the bay (Figure 3), an east-west gradient in snow depth could have been expected
474 over the rest of the bay. However, this gradient cannot be determined on average over the entire time series. This is mainly
475 due to temporary local disturbance factors in the bay, such as icebergs and pressure ridges, which locally dominate the snow
476 distribution and thus lead to a comparatively homogeneous distribution of snow depth over the central part of Atka Bay. A

477 south-north survey across the bay at the beginning of austral summer 2018, however, revealed a trend of decreasing snow
478 depth towards the northern fast-ice edge, with a stronger gradient approx. 5 km from the ice edge (Figure 7), which is in line
479 with the northern boundary of the ice-shelf edge (Figure 1) and can therefore be explained by associated decreasing offshore
480 winds and consequently less snow redistribution.

481 Due to the generally thick snow cover on Antarctic sea ice (Kern and Ozsoy-Çiçek, 2016; Markus and Cavalieri, 1998;
482 Massom et al., 2001b), flooding of the snow/ice interface and the resulting formation of snow-ice is a widespread
483 phenomenon in the Southern Ocean and contributes significantly to the sea-ice mass budget in the area (Eicken et al., 1995;
484 Jeffries et al., 2001). While Günther and Dieckmann (1999) observed no flooding in Atka Bay during their study, Kipfstuhl
485 (1991) reported flooding in relation to snow loads greater than 1 meter, an observation that we can largely confirm with our
486 data. Exceptions are measurements on comparatively thin ice that already showed a sufficient snow layer, e.g. in the austral
487 winter 2010 and 2011 at ATKA21, leading to a negative freeboard and potential flooding already early in the season (Figure
488 5). Consequently, taking all conducted freeboard measurements on the seasonal fast ice into account, 55 % of the data
489 indicate a negative freeboard, i.e. potential flooding and associated snow-ice formation can be assumed. While the snow
490 cover reduces the buoyancy of the sea ice and accelerates flooding, the underlying platelet layer counteracts this by adding
491 additional buoyancy. However, neglecting the platelet layer reduces the freeboard by 0.09 ± 0.06 m, but still a negative
492 freeboard is derived in half of the calculations. Thus, the spatial distribution of the sign of the freeboard, and therefore also
493 the flooding of the snow/ice interface, is essentially controlled by the snow layer on top of the fast ice in Atka Bay. The
494 thickness of the underlying platelet layer below in turn contributes to the resulting thickness of the flooded layer and
495 consequently to the thickness of the expected snow-ice layer.

496 **4.3 Impact of local disturbances on bay-wide properties and processes**

497 As already stated above, the largest overall effect on the fast-ice properties, the underlying platelet layer and the snow on top
498 is due to the presence of icebergs in front of Atka Bay, which might entirely prevent a fast-ice breakup. At the same time,
499 those grounded icebergs that are enclosed by sea ice within the bay add strong local effects. Thus, the large iceberg B15G
500 grounded in front of Atka Bay sheltering the fast ice in the bay and consequently preventing sea-ice breakup in the following
501 summer (Hoppmann et al., 2015b) led to second-year fast ice in the bay in 2013. Our measurements have shown that this
502 hardly had any effect on the monthly snow accumulation rate and platelet-layer growth rate, but rather that these were within
503 the same range as in the years of seasonal sea-ice cover. Accordingly, for perennial sea ice, the total annual snow and
504 platelet-layer thicknesses are approximately twice as thick as in the other years and average to 1.30 ± 0.60 m and 7.84 ± 1.33
505 m, respectively. Higher snow loads do also increase the probability and extent of surface flooding. This is not only observed
506 for years of perennial sea ice, but also for local disturbances as a result of the presence of small icebergs inside of the bay. In
507 contrast, the perennial fast-ice thickness is not as linear: Considering the large sea-ice thickness of around 2 m, as well as the
508 insulating effect of the thick snow cover on top, the contribution of congelation growth is very limited. Instead, it is highly
509 likely that dynamical growth as well as growth related to the consolidation of the platelet layer dominates the thickening of

510 the perennial fast ice, adding up to an average thickness of 4.19 ± 1.90 m, which is even more than double the thickness of
511 seasonal sea ice in the bay.

512

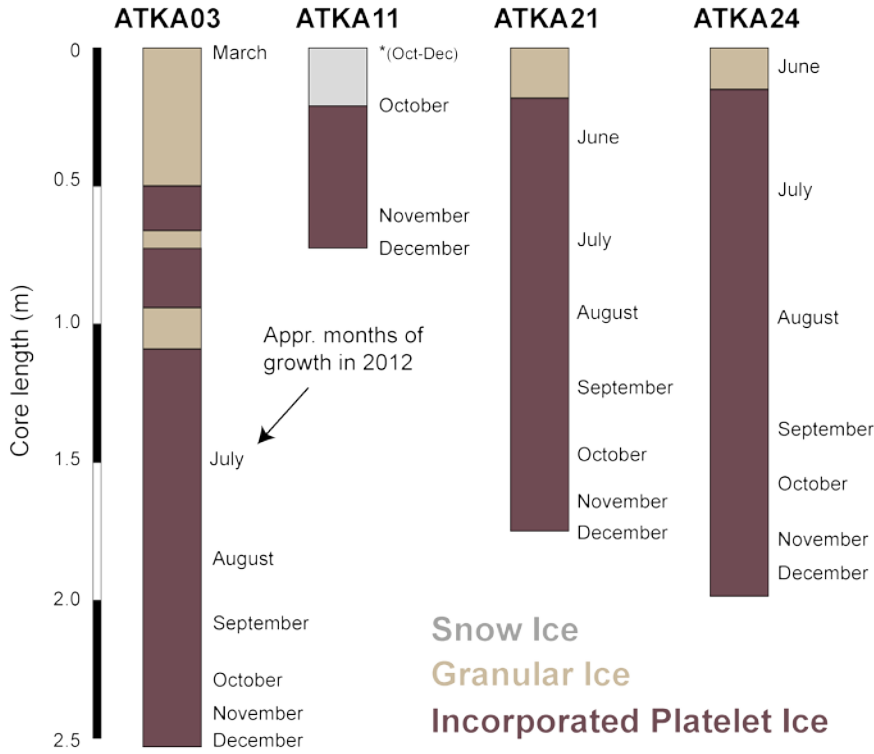
513 **4.4 Sea-ice growth history**

514 A detailed study of sea ice crystal fabric by means of visual inspection of thick/thin sections or with the help of an automated
515 fabric analyzer can help immensely to determine the dominant growth processes in a given area of interest. At the same time,
516 the growth history of fast ice is to a large degree governed by the timing of the formation of a persistent ice cover, and can
517 only be interpreted accurately by the help of as much auxiliary information as possible, most importantly from regular
518 satellite imagery such as MODIS, Sentinel-1 or Radarsat.

519 It has been planned since the start of the AFIN monitoring at Atka Bay in 2010 to regularly obtain sea ice cores for crystal
520 fabric analysis. A set of cores from the six main sampling sites (Figure 1) has been obtained in 2011, and again in 2012.
521 Only 4 out of these 12 cores have been processed so far (all from 2012), which is obviously only a very small sample size
522 compared to the decade of measurements shown above. While the limited ice core data thereby is insufficient to make
523 general statements about sea ice growth processes at Atka Bay, we provide this data here to highlight a few major aspects,
524 some of which have already been discussed earlier.

525 From the (limited) data we have from the four 2012 cores (Figure 9), it is evident that 1. there is no columnar texture at all;
526 2. there is a small fraction of granular ice in the top parts of three cores; 3. there is a small fraction of snow ice in one core
527 and 4. all cores are dominated by incorporated platelet ice. The core from the western part of Atka Bay (ATKA03) exhibits a
528 comparably high fraction of granular ice: a 0.5m long section at the top, and 2 smaller sections a little bit deeper, with some
529 incorporated platelet ice in between. This crystal fabric is a manifestation of the dynamic conditions under which the initial
530 growth takes place, and supports the other datasets shown above. The strong easterly winds (Figure 3) keep pushing the
531 initially forming thin ice towards the western ice shelf edge, which leads to a grinding of the fragile frazil crystals, and
532 subsequently to a rafting of the newly formed ice. This process seems to be still relevant even after the ice has thickened to
533 >0.5 m, probably by very strong winds. In this way, the thickening rate of the sea ice is greatly accelerated initially (Figure
534 4). The absence of exclusively columnar ice is evidence that there are already platelet crystals emerging from the cavity very
535 early in the season. While it has been suggested in an earlier study that such crystals would be present in the bay from June
536 onwards (Hoppmann et al., 2015b), there is a possibility that they might arrive even earlier, at least in parts of the bay close
537 to the outflow of ISW. While the ice core taken at ATKA11 is not representative at all for sea ice in the bay due to an early
538 breakup event and subsequent late refreezing, the presence of snow ice is an evidence for a process that we would argue
539 plays an underestimated role in this region. However, we currently do not have any more direct evidence for the wide
540 presence of snow ice at Atka Bay (due to the lack of ice core data) other than the observations of negative freeboard in our
541 main dataset (Figure 5), and several observations of extensive surface flooding from summer campaigns. In order to fill this
542 knowledge gap, a dedicated program of obtaining much more core sections from the top of the sea ice at different locations

543 would have to be implemented, with a subsequent crystal fabric and/or oxygen isotope analysis. As indicated above, this is
 544 currently not feasible. The other ice cores taken at ATKA21 and ATKA24 are close to the “typical” sea ice thickness at Atka
 545 Bay of 2 m, and exhibit the expected granular ice at the top from wind and waves, and incorporated platelet ice throughout
 546 the rest of the core. No evidence from dynamic growth processes is found in these cores. This is in line with our knowledge
 547 so far, especially since the sea ice in that area of the bay typically forms later in the year and is less influenced by strong
 548 winds.
 549

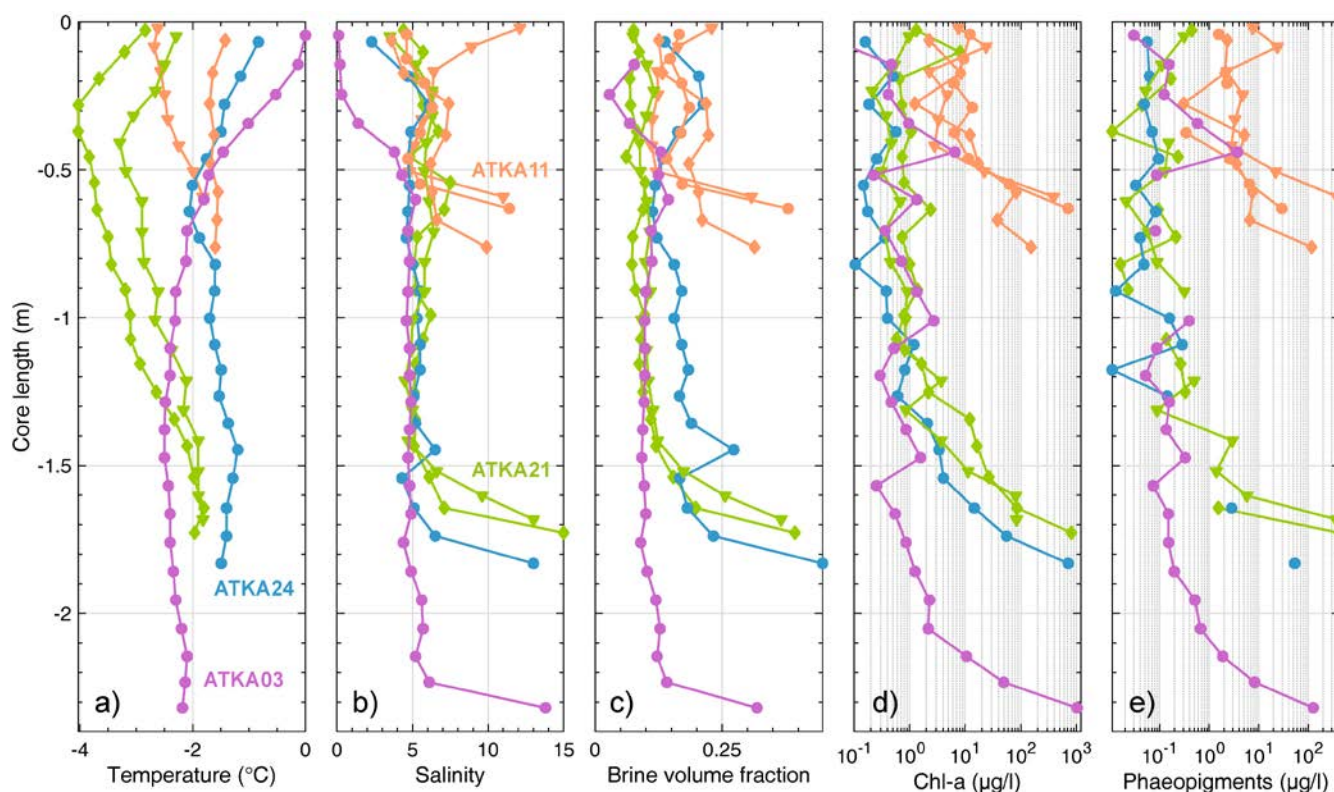


550
 551 **Figure 9:** Sea-ice crystal fabric from ice cores obtained at four different fast ice sampling sites in December 2012, derived
 552 from vertical and horizontal thin sections (0.1m spacing) along the full core length (see also Hoppmann et al., 2015a;
 553 Hoppmann et al., 2015b; Hoppmann, 2015).

554
 555 **4.5 Implications for multi-disciplinary research**

556 Such a multi-layered, thick sea-ice cover not only very efficiently separates the atmosphere from the ocean with respect to
 557 ice growth, but it also influences the exchange of any fluxes between the two climate system components. Thereby, it also
 558 strongly impacts the ice-associated ecosystem, which is particularly unique in sub-ice platelet layers (Arrigo, 2014). Günther

559 and Dieckmann (1999) concluded from their study that about 99% of the total fast-ice biomass in Atka Bay originates from
 560 algae initially growing in the sub-ice platelet layer. The maximum Chl-a concentration in their study was around 490 mg m^{-3}
 561 in the bottom of the fast ice, and 240 mg m^{-3} in the platelet layer in summer, at a site that had up to 0.35 m of snow cover.
 562 The authors argued that their total observed fast ice biomass was significantly lower compared to the mostly snow-free fast
 563 ice of the Ross Sea. However, it was still on the very upper range of biomass usually found in Antarctic fast ice (Meiners et
 564 al., 2018). At the same time, more recent results from 2012 reveal that Chl-a concentrations can reach up to 900 mg m^{-3}
 565 when there is much less snow present (Fig. 9).
 566



567
 568 **Figure 10:** Sea-ice physical and biological properties from cores obtained at different fast ice sampling sites in Nov/Dec
 569 2012 (after Hoppmann et al., 2013).
 570

571 While a few studies exist that investigate shade-adaptation in algae and link algal growth to snow depth on McMurdo Sound
 572 fast ice (e.g. Sullivan et al., 1985; McGrath Grossi et al., 1987; Robinson et al., 1995), so far still comparably little is known
 573 about the adaptation of the ecosystem in the upper ocean to perennial fast-ice conditions and sub-ice platelet layers. These
 574 and similar knowledge gaps that exist with respect to ice-shelf influenced fast-ice regimes can only be addressed by

575 integrated, multi-disciplinary research in comparably easy to access locations in coastal Antarctica, one of which was
576 introduced in this physical study.

577 **5 Conclusions**

578 This study presents a unique, 9-year long record (2010 to 2018) of snow depth, freeboard, sea-ice and sub-ice platelet-layer
579 thickness observed at Atka Bay, a coastal Antarctic fast-ice regime in the southeastern Weddell Sea and key region in the
580 Southern Ocean. As one of the longest time series within the Antarctic Fast Ice Network, and complementary to similar
581 records in the Ross Sea (Brett et al., 2020; Langhorne et al., 2015 and references therein), this dataset is expected to serve as
582 an important baseline in the context of climate change and future sea-ice evolution in this region, and will contribute to an
583 enhanced understanding of the complex interactions between the atmosphere, sea ice, ocean and ice shelves in the Southern
584 Ocean.

585 For the period of the study presented, and considering individual observations from the 1980s and 1990s, a predominantly
586 seasonal character of the fast-ice regime in Atka Bay is evident without a noticeable trend for any of the analyzed variables.
587 The absence of any trend and the seasonality of surface characteristics associated with the year-round snow cover and
588 negligible surface melting coincides with the prevailing conditions in the Antarctic pack-ice zone. Hence, the described
589 observations in Atka Bay over the last nine years not only allow to document a baseline of the observed parameters, but also
590 to capture processes and properties prior to expected future changes of pack ice in, e.g., the Weddell Sea, due to a changing
591 climate.

592 Atka Bay is dominated by strong cyclonic events leading to easterly winds which determine not only the freeze-up of the bay
593 in autumn and breakup during summer months, but also govern the year-round snow redistribution on the ice. The
594 consequent substantial annual snow accumulation determines both, the magnitude and duration of congelation sea-ice
595 growth, as well as the magnitude and spatial distribution of the frequent negative freeboard and related flooding of the
596 snow/ice interface, and thus subsequent snow-ice formation. In contrast, platelet ice contributes significantly to the total sea-
597 ice mass balance in this region, both, in its unconsolidated form as an underlying (buoyant) platelet layer, as well as through
598 its incorporation into the solid sea ice (see also Hoppmann et al., 2015a; Hoppmann et al., 2015b). However, our results
599 indicate that, although the platelet layer partly offsets the negative freeboard, it is not buoyant enough to lift the snow/ice
600 interface above sea level against the weight of the prevalent snow.

601 With regard to the platelet layer and its formation process, we conclude that, although the annual platelet-layer thickness
602 increase of four meters seems to be independent of the age of the fast ice in the bay, the seasonal and inter-annual variability
603 of this layer and thus the associated ocean properties and processes cannot be understood sufficiently by just considering the
604 fast-ice properties alone. We therefore recommend to follow the approach of the New Zealand research program at Scott
605 Base to generally include an oceanographic component into any fast-ice monitoring, especially in regions where ice shelves
606 are present. This combination would allow for quantifying the seasonal interactions between sea ice, ocean and shelf ice

607 even more precisely and thus to better understand current patterns and accumulation rates of platelet ice and associated
608 biomass under the ice as a function of the distance to the shelf-ice and sea-ice edge. These results would provide a solid basis
609 to be applied to all fast-ice areas around Antarctica, and thus make a fundamental contribution to the understanding of the
610 Antarctic climate system.

611 **Data availability**

612 All presented meteorological data are archived in PANGAEA at <https://doi.pangaea.de/10.1594/PANGAEA.908826>. All
613 fast-ice data are archived in PANGAEA at <https://doi.pangaea.de/10.1594/PANGAEA.908860>.

614 **Author contribution**

615 SA conducted most of the analyses for this paper and did the main writing with input from all co-authors. MH contributed
616 the sea ice core data and performed the revision with input from all other authors. MN is the principal investigator of the
617 AFIN work at Neumayer III. MH, MN and SA supervised the sea-ice measurements of the overwintering teams during the
618 study period. MH and SA participated in field campaigns to collect parts of the presented data. HS contributed the
619 meteorological datasets and the related analysis. AF contributed the fast-ice extent dataset and the related analysis.

620 **Competing interests**

621 The authors declare that they have no conflict of interest.

622 **Acknowledgements**

623 We are most grateful to the overwintering teams at Neumayer III from 2010 to 2018 for their conducted measurements on
624 the fast ice in Atka Bay. Special thanks are due to the respective meteorologists of the teams who led the sea ice work on
625 site. Also, our work and research at Neumayer III would not have been possible without the extensive support of the AWI
626 logistics. We also acknowledge the scientific support of Christian Haas, the logistical support of Anja Nicolaus, and the
627 technical support of Jan Rohde, all from the Sea Ice Physics section at AWI. This work was supported by the German
628 Research Council (DFG) in the framework of the priority programme ‘‘Antarctic Research with comparative investigations
629 in Arctic ice areas’’ by grants to SPP1158, HE2740/12, NI1092/2 and AR1236/1, and the Alfred-Wegener-Institut
630 Helmholtz-Zentrum für Polar- und Meeresforschung. This research was also supported under Australian Research Council's
631 Special Research Initiative for Antarctic Gateway Partnership (Project ID SR140300001). We are grateful to two anonymous
632 reviewers for their valuable input, which significantly improved the quality of the presented science.

633 **References**

- 634 Aoki, S.: Breakup of land-fast sea ice in Lützow-Holm Bay, East Antarctica, and its teleconnection to tropical Pacific sea
635 surface temperatures, *Geophysical research letters*, 44, 3219-3227, 2017.
- 636 Arndt, S., Willmes, S., Dierking, W., and Nicolaus, M.: Timing and regional patterns of snowmelt on Antarctic sea ice from
637 passive microwave satellite observations, *Journal of Geophysical Research - Oceans*, 121, 5916-5930,
638 10.1002/2015JC011504, 2016.
- 639 Arndt, S., Asseng, J., Behrens, L. K., Hoppmann, M., Hunkeler, P. A., Ludewig, E., Müller, H., Paul, S., Rau, A., Schmidt,
640 T., Schmithüsen, H., Schulz, H., Stautzebach, E., and Nicolaus, M.: Thickness and properties of sea ice and snow of land-
641 fast sea ice in Atka Bay in 2010-2018, reference list of 9 datasets, Alfred Wegener Institute, Helmholtz Centre for Polar and
642 Marine Research, Bremerhaven, PANGAEA, <https://doi.pangaea.de/10.1594/PANGAEA.908860>, 2019.
- 643 Arrigo, K. R.: Sea ice ecosystems, *Ann Rev Mar Sci*, 6, 439-467, 10.1146/annurev-marine-010213-135103, 2014.
- 644 Boebel, O., Kindermann, L., Klinck, H., Bornemann, H., Plötz, J., Steinhage, D., Riedel, S., and Burkhardt, E.: Real-time
645 underwater sounds from the Southern Ocean, *Eos transactions*, 87, 361,366, 2006.
- 646 Brett, G. M., Irvin, A., Rack, W., Haas, C., Langhorne, P. J., and Leonard, G. H.: Variability in the Distribution of Fast Ice
647 and the Sub-ice Platelet Layer Near McMurdo Ice Shelf, *Journal of Geophysical Research: Oceans*, 125, e2019JC015678,
648 10.1029/2019jc015678, 2020.
- 649 Dammann, D. O., Eriksson, L. E. B., Mahoney, A. R., Eicken, H., and Meyer, F. J.: Mapping pan-Arctic landfast sea ice
650 stability using Sentinel-1 interferometry, *The Cryosphere*, 13, 557-577, 10.5194/tc-13-557-2019, 2019.
- 651 Dempsey, D. E., Langhorne, P. J., Robinson, N. J., Williams, M. J. M., Haskell, T. G., and Frew, R. D.: Observation and
652 modeling of platelet ice fabric in McMurdo Sound, Antarctica, *Journal of Geophysical Research-Oceans*, 115, Artn C01007
653 Doi 10.1029/2008jc005264, 2010.
- 654 Divine, D., Korsnes, R., and Makshtas, A.: Variability and climate sensitivity of fast ice extent in the north-eastern Kara Sea,
655 *Polar Research*, 22, 27-34, 10.1111/j.1751-8369.2003.tb00092.x, 2003.
- 656 Druckenmiller, M. L., Eicken, H., Johnson, M. A., Pringle, D. J., and Williams, C. C.: Toward an integrated coastal sea-ice
657 observatory: System components and a case study at Barrow, Alaska, *Cold Regions Science and Technology*, 56, 61-72,
658 10.1016/j.coldregions.2008.12.003, 2009.
- 659 Eicken, H., and Lange, M. A.: Development and properties of sea ice in the coastal regime of the southeastern Weddell Sea,
660 *Journal of Geophysical Research: Oceans*, 94, 8193-8206, 10.1029/JC094iC06p08193, 1989.
- 661 Eicken, H., Lange, M. A., Hubberten, H. W., and Wadhams, P.: Characteristics and distribution patterns of snow and
662 meteoric ice in the Weddell Sea and their contribution to the mass balance of sea ice, *Annales Geophysicae-Atmospheres*
663 *Hydrospheres and Space Sciences*, 12, 80-93, 10.1007/s00585-994-0080-x, 1994.
- 664 Eicken, H., Fischer, H., and Lemke, P.: Effects of the snow cover on Antarctic sea ice and potential modulation of its
665 response to climate change, *Annals of Glaciology*, 21, 369-376, 1995.
- 666 Foldvik, A. a. K., T. : Thermohaline convection in the vicinity of an ice shelf, in: *Polar oceans, Proceedings of the Polar*
667 *Oceans Conference held at McGill University, Montreal, May, 1974*, edited by: Dunbar, M. J., Arctic Institute of North
668 America, Calgary, Alberta, 247-255, 1977.

- 669 Fraser, A. D., Massom, R. A., Michael, K. J., Galton-Fenzi, B. K., and Lieser, J. L.: East Antarctic landfast sea ice
670 distribution and variability, 2000–08, *Journal of Climate*, 25, 1137-1156, 2012.
- 671 Fraser, A. D., Ohshima, K. I., Nihashi, S., Massom, R. A., Tamura, T., Nakata, K., Williams, G. D., Carpentier, S., and
672 Willmes, S.: Landfast ice controls on sea-ice production in the Cape Darnley Polynya: A case study, *Remote Sensing of*
673 *Environment*, 233, 111315, 2019.
- 674 Galley, R. J., Else, B. G. T., Howell, S. E. L., Lukovich, J. V., and Barber, D. G.: Landfast Sea Ice Conditions in the
675 Canadian Arctic: 1983-2009, *Arctic*, 65, 133-144, 2012.
- 676 Giles, A. B., Massom, R. A., and Lytle, V. I.: Fast-ice distribution in East Antarctica during 1997 and 1999 determined using
677 RADARSAT data, *Journal of Geophysical Research: Oceans*, 113, 2008.
- 678 Gough, A. J., Mahoney, A. R., Langhorne, P. J., Williams, M. J. M., Robinson, N. J., and Haskell, T. G.: Signatures of
679 supercooling: McMurdo Sound platelet ice, *Journal of Glaciology*, 58, 38-50, Doi 10.3189/2012jog10j218, 2012.
- 680 Grosfeld, K., Treffeisen, R., Asseng, J., Bartsch, A., Bräuer, B., Fritsch, B., Gerdes, R., Hendricks, S., Hiller, W., and
681 Heygster, G.: Online sea-ice knowledge and data platform < [www. meereisportal. de](http://www.meereisportal.de) >, *Polarforschung*, 85, 143-155, 2015.
- 682 Günther, S., and Dieckmann, G. S.: Seasonal development of algal biomass in snow-covered fast ice and the underlying
683 platelet layer in the Weddell Sea, Antarctica, *Antarct Sci*, 11, 305-315, 1999.
- 684 Günther, S., and Dieckmann, G. S.: Vertical zonation and community transition of sea-ice diatoms in fast ice and platelet
685 layer, Weddell Sea, Antarctica, in: *Ann Glaciol*, edited by: Jeffries, M. O., and Eicken, H., *Annals of Glaciology*, Int
686 *Glaciological Soc*, Cambridge, 287-296, 2001.
- 687 Haas, C.: The seasonal cycle of ERS scatterometer signatures over perennial Antarctic sea ice and associated surface ice
688 properties and processes, *Ann Glaciol*, 33, 69-73, 10.3189/172756401781818301, 2001.
- 689 Haas, C., Thomas, D. N., and Bareiss, J.: Surface properties and processes of perennial Antarctic sea ice in summer, *Journal*
690 *of Glaciology*, 47, 613-625, 10.3189/172756501781831864, 2001.
- 691 Hattermann, T., Nøst, O. A., Lilly, J. M., and Smedsrud, L. H.: Two years of oceanic observations below the Fimbul Ice
692 Shelf, Antarctica, *Geophysical Research Letters*, 39, 2012.
- 693 Heil, P.: Atmospheric conditions and fast ice at Davis, East Antarctica: A case study, *Journal of Geophysical Research:*
694 *Oceans*, 111, 2006.
- 695 Heil, P., Gerland, S., and Granskog, M.: An Antarctic monitoring initiative for fast ice and comparison with the Arctic, *The*
696 *Cryosphere Discussions*, 5, 2437-2463, 2011.
- 697 Hoppmann, M., Paul, S., Hunkeler, P., Baltés, U., Kühnel, M., Schmidt, T., Nicolaus, M., Heinemann, G., and Willmes, S.:
698 Field work on Atka Bay land-fast sea ice in 2012/13. 2013.
- 699 Hoppmann, M.: *Sea-Ice Mass Balance Influenced by Ice Shelves*, Jacobs University Bremen, 2015.
- 700 Hoppmann, M., Nicolaus, M., Hunkeler, P. A., Heil, P., Behrens, L. K., König-Langlo, G., and Gerdes, R.: Seasonal
701 evolution of an ice-shelf influenced fast-ice regime, derived from an autonomous thermistor chain, *Journal of Geophysical*
702 *Research-Oceans*, 120, 1703-1724, 10.1002/2014jc010327, 2015a.

- 703 Hoppmann, M., Nicolaus, M., Paul, S., Hunkeler, P. A., Heinemann, G., Willmes, S., Timmermann, R., Boebel, O., Schmidt,
704 T., Kuhnel, M., König-Langlo, G., and Gerdes, R.: Ice platelets below Weddell Sea landfast sea ice, *Annals of Glaciology*,
705 56, 175-190, 10.3189/2015AoG69A678, 2015b.
- 706 Hoppmann, M. R., M. E. ; Smith, I. J.; Jendersie, S.; Langhorne, P. J.; Thomas, D. N.; Dieckmann, G. S.: Platelet ice, the
707 Southern Ocean's hidden ice: a review, *Annals of Glaciology*, 61, in review.
- 708 Hughes, K. G., Langhorne, P. J., Leonard, G. H., and Stevens, C. L.: Extension of an Ice Shelf Water plume model beneath
709 sea ice with application in McMurdo Sound, Antarctica, *Journal of Geophysical Research: Oceans*, 119, 8662-8687,
710 10.1002/2013jc009411, 2014.
- 711 Hunkeler, P. A., Hoppmann, M., Hendricks, S., Kalscheuer, T., and Gerdes, R.: A glimpse beneath Antarctic sea ice: Platelet
712 layer volume from multifrequency electromagnetic induction sounding, *Geophysical Research Letters*, 43, 222-231, 2016.
- 713 Jacobs, S., Helmer, H., Doake, C., Jenkins, A., and Frolich, R.: Melting of ice shelves and the mass balance of Antarctica,
714 *Journal of Glaciology*, 38, 375-387, 1992.
- 715 JCOMM Expert Team on Sea Ice: WMO Sea-Ice Nomenclature I-III, 2015.
- 716 Jeffries, M., Li, S., Jana, R., Krouse, H., and Hurst-Cushing, B.: Late winter first-year ice floe thickness variability, seawater
717 flooding and snow ice formation in the Amundsen and Ross Seas, *Antarctic Sea Ice: Physical processes, interactions and
718 variability*, 74, 69-87, 1998.
- 719 Jeffries, M. O., Krouse, H. R., Hurst-Cushing, B., and Maksym, T.: Snow-ice accretion and snow-cover depletion on
720 Antarctic first-year sea-ice floes, *Annals of Glaciology*, 33, 51-60, 2001.
- 721 Kawamura, T., Jeffries, M. O., Tison, J.-L., and Krouse, H. R.: Superimposed-ice formation in summer on Ross Sea pack-ice
722 floes, *Annals of glaciology*, 39, 563-568, 2004.
- 723 Kern, S., and Ozsoy-Çiçek, B.: Satellite Remote Sensing of Snow Depth on Antarctic Sea Ice: An Inter-Comparison of Two
724 Empirical Approaches, *Remote Sensing*, 8, 450, 10.3390/rs8060450, 2016.
- 725 Kipfstuhl, J.: Zur Entstehung von Unterwassereis und das Wachstum und die Energiebilanz des Meereises in der Atka
726 Bucht, Antarktis= On the formation of underwater ice and the growth and energy budget of the sea ice in Atka Bay,
727 Antarctica, *Berichte zur Polarforschung (Reports on Polar Research)*, 85, 1991.
- 728 König-Langlo, G., and Loose, B.: The Meteorological Observatory at Neumayer Stations (GvN and NM-II) Antarctica,
729 *Berichte zur Polar-und Meeresforschung (Reports on Polar and Marine Research)*, 76, 25-38, 2007.
- 730 Kwok, R., Pang, S. S., and Kacimi, S.: Sea ice drift in the Southern Ocean: Regional patterns, variability, and trends, *Elem
731 Sci Anth*, 5, 2017.
- 732 Langhorne, P. J., Hughes, K. G., Gough, A. J., Smith, I. J., Williams, M. J. M., Robinson, N. J., Stevens, C. L., Rack, W.,
733 Price, D., Leonard, G. H., Mahoney, A. R., Haas, C., and Haskell, T. G.: Observed platelet ice distributions in Antarctic sea
734 ice: An index for ocean-ice shelf heat flux, *Geophysical Research Letters*, 42, 5442-5451, 10.1002/2015gl064508, 2015.
- 735 Lei, R. B., Li, Z. J., Cheng, B., Zhang, Z. H., and Heil, P.: Annual cycle of landfast sea ice in Prydz Bay, east Antarctica,
736 *Journal of Geophysical Research-Oceans*, 115, C02006, Artn C02006
737 Doi 10.1029/2008jc005223, 2010.

- 738 Lemieux, J. F., Dupont, F., Blain, P., Roy, F., Smith, G. C., and Flato, G. M.: Improving the simulation of landfast ice by
739 combining tensile strength and a parameterization for grounded ridges, *Journal of Geophysical Research: Oceans*, 121, 7354-
740 7368, 2016.
- 741 Leonard, G. H., Purdie, C. R., Langhorne, P. J., Haskell, T. G., Williams, M. J. M., and Frew, R. D.: Observations of platelet
742 ice growth and oceanographic conditions during the winter of 2003 in McMurdo Sound, Antarctica, *Journal of Geophysical
743 Research-Oceans*, 111, Artn C04012
744 Doi 10.1029/2005jc002952, 2006.
- 745 Leonard, G. H., Langhorne, P. J., Williams, M. J. M., Vennell, R., Purdie, C. R., Dempsey, D. E., Haskell, T. G., and Frew,
746 R. D.: Evolution of supercooling under coastal Antarctic sea ice during winter, *Antarct. Sci.*, 23, 399-409, Doi
747 10.1017/S0954102011000265, 2011.
- 748 Li, L., and Pomeroy, J. W.: Estimates of threshold wind speeds for snow transport using meteorological data, *J Appl
749 Meteorol*, 36, 205-213, 10.1175/1520-0450, 1997.
- 750 Mahoney, A., Eicken, H., Gaylord, A. G., and Shapiro, L.: Alaska landfast sea ice: Links with bathymetry and atmospheric
751 circulation, *Journal of Geophysical Research: Oceans*, 112, 2007a.
- 752 Mahoney, A., Eicken, H., and Shapiro, L.: How fast is landfast sea ice? A study of the attachment and detachment of
753 nearshore ice at Barrow, Alaska, *Cold Regions Science and Technology*, 47, 233-255, 10.1016/j.coldregions.2006.09.005,
754 2007b.
- 755 Mahoney, A. R., Gough, A. J., Langhorne, P. J., Robinson, N. J., Stevens, C. L., Williams, M. M. J., and Haskell, T. G.: The
756 seasonal appearance of ice shelf water in coastal Antarctica and its effect on sea ice growth, *Journal of Geophysical
757 Research-Oceans*, 116, Artn C11032
758 Doi 10.1029/2011jc007060, 2011.
- 759 Mahoney, A. R., Eicken, H., Gaylord, A. G., and Gens, R.: Landfast sea ice extent in the Chukchi and Beaufort Seas: The
760 annual cycle and decadal variability, *Cold Regions Science and Technology*, 103, 41-56,
761 <https://doi.org/10.1016/j.coldregions.2014.03.003>, 2014.
- 762 Markus, T., and Cavalieri, D. J.: Snow depth distribution over sea ice in the Southern Ocean from satellite passive
763 microwave data, *Antarctic sea ice: physical processes, interactions and variability*, 19-39, 1998.
- 764 Massom, R., Hill, K., Lytle, V., Worby, A., Paget, M., and Allison, I.: Effects of regional fast-ice and iceberg distributions
765 on the behaviour of the Mertz Glacier polynya, East Antarctica, *Annals of Glaciology*, 33, 391-398, 2001a.
- 766 Massom, R., Jacka, K., Pook, M., Fowler, C., Adams, N., and Bindoff, N.: An anomalous late-season change in the regional
767 sea ice regime in the vicinity of the Mertz Glacier Polynya, East Antarctica, *Journal of Geophysical Research: Oceans*, 108,
768 2003.
- 769 Massom, R. A., Eicken, H., Haas, C., Jeffries, M. O., Drinkwater, M. R., Sturm, M., Worby, A. P., Wu, X. R., Lytle, V. I.,
770 Ushio, S., Morris, K., Reid, P. A., Warren, S. G., and Allison, I.: Snow on Antarctic Sea ice, *Rev Geophys*, 39, 413-445,
771 10.1029/2000rg000085, 2001b.
- 772 Massom, R. A., Hill, K., Barbraud, C., Adams, N., Ancel, A., Emmerson, L., and Pook, M. J.: Fast ice distribution in Adélie
773 Land, East Antarctica: interannual variability and implications for emperor penguins *Aptenodytes forsteri*, *Marine Ecology
774 Progress Series*, 374, 243-257, 2009.

- 775 Massom, R. A., Giles, A. B., Fricker, H. A., Warner, R. C., Legrésy, B., Hyland, G., Young, N., and Fraser, A. D.:
 776 Examining the interaction between multi-year landfast sea ice and the Mertz Glacier Tongue, East Antarctica: Another factor
 777 in ice sheet stability?, *Journal of Geophysical Research: Oceans*, 115, 2010.
- 778 Massom, R. A., Scambos, T. A., Bennetts, L. G., Reid, P., Squire, V. A., and Stammerjohn, S. E.: Antarctic ice shelf
 779 disintegration triggered by sea ice loss and ocean swell, *Nature*, 558, 383-389, 10.1038/s41586-018-0212-1, 2018.
- 780 McGrath Grossi, S., Kottmeier, S. T., Moe, R. L., Taylor, G. T., and Sullivan, C. W.: Sea ice microbial communities – VI –
 781 Growth and primary production in bottom ice under graded snow cover, *Marine Ecology - Progress Series*, 35, 153-164,
 782 1987.
- 783 Meiners, K. M., Vancoppenolle, M., Carnat, G., Castellani, G., Delille, B., Delille, D., Dieckmann, G. S., Flores, H., Fripiat,
 784 F., Grotti, M., Lange, B. A., Lannuzel, D., Martin, A., McMinn, A., Nomura, D., Peeken, I., Rivaro, P., Ryan, K. G., Stefels,
 785 J., Swadling, K. M., Thomas, D. N., Tison, J. L., van der Merwe, P., van Leeuwe, M. A., Weldrick, C., and Yang, E. J.:
 786 Chlorophyll-a in Antarctic Landfast Sea Ice: A First Synthesis of Historical Ice Core Data, *Journal of Geophysical Research:*
 787 *Oceans*, 123, 8444-8459, 10.1029/2018JC014245, 2018.
- 788 Murphy, E. J., Clarke, A., Symon, C., and Priddle, J.: Temporal variation in Antarctic sea-ice: analysis of a long term fast-
 789 ice record from the South Orkney Islands, *Deep Sea Research Part I: Oceanographic Research Papers*, 42, 1045-1062, 1995.
- 790 Nicolaus, M., and Grosfeld, K.: Ice-Ocean Interactions underneath the Antarctic Ice Shelf Ekströmisen, *Polarforschung*, 72,
 791 17-29, 2004.
- 792 Olason, E.: A dynamical model of Kara Sea land-fast ice, *Journal of Geophysical Research-Oceans*, 121, 3141-3158,
 793 10.1002/2016JC011638, 2016.
- 794 Polyakov, I. V., Alekseev, G. V., Bekryaev, R. V., Bhatt, U. S., Colony, R., Johnson, M. A., Karklin, V. P., Walsh, D., and
 795 Yulin, A. V.: Long-Term Ice Variability in Arctic Marginal Seas, *Journal of Climate*, 16, 2078-2085, 10.1175/1520-
 796 0442(2003)016<2078:LIVIAM>2.0.CO;2, 2003.
- 797 Price, D., Rack, W., Langhorne, P. J., Haas, C., Leonard, G., and Barnsdale, K.: The sub-ice platelet layer and its influence
 798 on freeboard to thickness conversion of Antarctic sea ice, *Cryosphere*, 8, 1031-1039, DOI 10.5194/tc-8-1031-2014, 2014.
- 799 Robinson, D. H., Arrigo, K. R., Iturriaga, R., and Sullivan, C. W.: Microalgal Light-Harvesting in Extreme Low-Light
 800 Environments in Mcmurdo Sound, Antarctica1, *J. Phycol.*, 31, 508-520, 10.1111/j.1529-8817.1995.tb02544.x, 1995.
- 801 Robinson, N. J., Williams, M. J. M., Stevens, C. L., Langhorne, P. J., and Haskell, T. G.: Evolution of a supercooled Ice
 802 Shelf Water plume with an actively growing subice platelet matrix, *Journal of Geophysical Research-Oceans*, 119, 3425-
 803 3446, Doi 10.1002/2013jc009399, 2014.
- 804 Schmithüsen, H., König-Langlo, G., Müller, H., and Schulz, H.: Continuous meteorological observations at Neumayer
 805 station (2010-2018),reference list of 108 datasets, Alfred Wegener Institute, Helmholtz Centre for Polar and Marine
 806 Research, Bremerhaven, PANGAEA, <https://doi.pangaea.de/10.1594/PANGAEA.908826>, 2019.
- 807 Selyuzhenok, V., Krumpfen, T., Mahoney, A., Janout, M., and Gerdes, R.: Seasonal and interannual variability of fast ice
 808 extent in the southeastern Laptev Sea between 1999 and 2013, *Journal of Geophysical Research: Oceans*, n/a-n/a,
 809 10.1002/2015JC011135, 2015.
- 810 Selyuzhenok, V., Mahoney, A., Krumpfen, T., Castellani, G., and Gerdes, R.: Mechanisms of fast-ice development in the
 811 south-eastern Laptev Sea: a case study for winter of 2007/08 and 2009/10, *Polar Research*, 36, Artn 1411140

812 10.1080/17518369.2017.1411140, 2017.

813 Smith, E. C., Hattermann, T., Kuhn, G., Gaedicke, C., Berger, S., Drews, R., Ehlers, T. A., Franke, D., Gromig, R.,
814 Hofstede, C., Lambrecht, A., Läufer, A., Mayer, C., Tiedemann, R., Wilhelms, F., and Eisen, O.: Detailed Seismic
815 Bathymetry Beneath Ekström Ice Shelf, Antarctica: Implications for Glacial History and Ice-Ocean Interaction, *Geophysical*
816 *Research Letters*, 47, e2019GL086187, 10.1029/2019gl086187, 2020.

817 Smith, I. J., Langhorne, P. J., Frew, R. D., Vennell, R., and Haskell, T. G.: Sea ice growth rates near ice shelves, *Cold*
818 *Regions Science and Technology*, 83-84, 57-70, 10.1016/j.coldregions.2012.06.005, 2012.

819 Sullivan, C. W., Palmisano, A. C., Kottmeier, S., Grossi, S. M., and Moe, R.: The Influence of Light on Growth and
820 Development of the Sea-Ice Microbial Community of McMurdo Sound, in: *Antarctic Nutrient Cycles and Food Webs*,
821 edited by: Siegfried, W., Condy, P., and Laws, R., Springer Berlin Heidelberg, 78-83, 1985.

822 Tamura, T., Williams, G., Fraser, A., and Ohshima, K.: Potential regime shift in decreased sea ice production after the Mertz
823 Glacier calving, *Nature communications*, 3, 826, 2012.

824 Tamura, T., Ohshima, K. I., Fraser, A. D., and Williams, G. D.: Sea ice production variability in Antarctic coastal polynyas,
825 *Journal of Geophysical Research: Oceans*, 121, 2967-2979, 2016.

826 Williams, G., Bindoff, N., Marsland, S., and Rintoul, S.: Formation and export of dense shelf water from the Adélie
827 Depression, East Antarctica, *Journal of Geophysical Research: Oceans*, 113, 2008.

828 Yu, Y., Stern, H., Fowler, C., Fetterer, F., and Maslanik, J.: Interannual Variability of Arctic Landfast Ice between 1976 and
829 2007, *Journal of Climate*, 27, 227-243, 10.1175/jcli-d-13-00178.1, 2014.

830